EPRI | ELECTRIC POWER RESEARCH INSTITUTE

Materials Reliability Program: Evaluation of Risk from Carbon Macrosegregation in Reactor Pressure Vessel and Other Large Nuclear Forgings (MRP-417)

2017 TECHNICAL REPORT

Materials Reliability Program: Evaluation of Risk from Carbon Macrosegregation in Reactor Pressure Vessel and Other Large Nuclear Forgings (MRP-417)

3002010331

Final Report, June 2017

EPRI Project Manager
T. Hardin

ELECTRIC POWER RESEARCH INSTITUTE
3420 Hillview Avenue, Palo Alto, California 94304-1338 ▪ PO Box 10412, Palo Alto, California 94303-0813 ▪ USA
800.313.3774 ▪ 650.855.2121 ▪ askepri@epri.com ▪ www.epri.com

DISCLAIMER OF WARRANTIES AND LIMITATION OF LIABILITIES

THE FOLLOWING ORGANIZATION, UNDER CONTRACT TO EPRI, PREPARED THIS REPORT:

Sartrex Corporation

NOTE

For further information about EPRI, call the EPRI Customer Assistance Center at 800.313.3774 or e-mail askepri@epri.com.

ACKNOWLEDGMENTS

The following organization, under contract to the Electric Power Research Institute (EPRI), prepared this report:

Sartrex Corporation
1700 Rockville Pike
Suite 400
Rockville, MD 20852

Principal Investigator
R. Gamble

This report describes research sponsored by EPRI.

This publication is a corporate document that should be cited in the literature in the following manner:

Materials Reliability Program: Evaluation of Risk from Carbon Macrosegregation in Reactor Pressure Vessel and Other Large Nuclear Forgings (MRP-417). EPRI, Palo Alto, CA: 2017. 3002010331.

PRODUCT DESCRIPTION

In 2014, carbon macrosegregation was identified in pressurized water reactor (PWR) pressure vessel head forgings in France. This report assesses the generic implications of that discovery for large forged, pressure retaining components in PWRs.

Background

Regions of higher-than-normal carbon due to macrosegregation during the cooling of large conventional ingots have been found or are suspected to have the potential for being present in various large forged, ferritic pressure retaining components in PWRs. Large forgings may be used for reactor pressure vessel (RPV) shell rings and monoblock heads, steam generator (S/G) shell rings and bottom channel heads, and pressurizer shells and heads. Macrosegregation causes localized areas within a large forging to have carbon concentrations higher than the surrounding, bulk material. In shell rings, levels 25% higher than normal have been measured; in some S/G channel heads in France, levels 100% higher have been measured. Carbon affects ferritic steel by increasing strength but decreasing toughness; therefore, localized areas of low toughness may exist in forgings with excessive carbon macrosegregation. Until now, the safety significance of potential high carbon, low-toughness areas in a large nuclear forging has not received significant study.

Challenges and Objectives

The objective of this project is to evaluate the safety significance of postulated carbon macrosegregation in large forgings that are often used in the primary pressure boundary of a PWR.

Approach

The Materials Reliability Program (MRP) conducted bounding probabilistic fracture mechanics (PFM) analyses to assess the structural significance of postulated carbon macrosegregation in large forged, pressure retaining components in PWRs. The approach for these analyses is consistent with analyses for pressurized thermal shock (PTS) transients performed by the Nuclear Regulatory Commission (NRC) staff in development of the Alternate PTS Rule, 10CFR50.61a.

Results and Findings

MRP performed a bounding safety assessment for forged components postulated to have high carbon due to excessive macrosegregation. The components included in the evaluation are RPV beltline and nozzle shell course ring forgings, RPV head forgings, and pressurizer and steam generator (S/G) ring and head forgings. The bounding assessment included a PFM analysis of the material with the highest mean reference temperature in a beltline ring forging in the U.S. PWR fleet at the end of an 80-year operating interval. The results from the assessment indicate that the risk associated with the presence of carbon macrosegregation in PWR ring and head forgings is

significantly lower than current regulatory risk related criteria, and acceptable margins against failure would be maintained even if carbon macrosegregation were to be present in the large forgings used in the primary pressure boundary of PWRs.

Applications, Value, and Use

Results of this work demonstrate that components with postulated carbon macrosegregation continue to meet applicable regulatory safety risk criteria through an 80-year operating interval.

Keywords

PWR
Carbon macrosegregation
Head and ring forgings
Forged component structural integrity
Pressurized thermal shock

Deliverable Number: 3002010331

Product Type: Technical Report

Materials Reliability Program: Evaluation of Risk from Carbon Macrosegregation in Reactor Pressure Vessel and Other Large Nuclear Forgings (MRP-417)

PRIMARY AUDIENCE: Engineers addressing issues related to high carbon due to macrosegregation in ferritic pressure boundary components.

KEY RESEARCH QUESTION

Regions of higher-than-normal carbon due to macrosegregation during the cooling of large conventional ingots have been found or are suspected to be present in various large forged, ferritic pressure retaining components in PWRs. Large forgings may be used for reactor pressure vessel (RPV) shell rings and monoblock heads, steam generator (S/G) shell rings and bottom channel heads, and pressurizer shells and heads. Macrosegregation causes localized areas within a large forging to have carbon concentrations higher than the surrounding, bulk material. In ring forgings, levels 25% higher than normal have been measured; in some S/G channel heads in France, levels 100% higher have been measured. Carbon affects ferritic steel by increasing strength but decreasing the toughness; therefore, localized areas of low toughness may exist in forgings with excessive carbon macrosegregation.

RESEARCH OVERVIEW

The objective of this project was to evaluate the safety significance of postulated carbon macrosegregation in large forgings that are often used in the primary pressure boundary of a PWR. The Materials Reliability Program (MRP) conducted bounding probabilistic fracture mechanics (PFM) analyses to assess the structural significance of postulated carbon macrosegregation in large forged, pressure retaining components in PWRs. The approach for these analyses is consistent with analyses for pressurized thermal shock (PTS) transients performed by the Nuclear Regulatory Commission (NRC) staff in development of the Alternate PTS Rule, 10CFR50.61a. The components included in the evaluation are RPV beltline and nozzle shell course ring forgings, RPV head forgings, and pressurizer and S/G ring and head forgings. The bounding assessment included a PFM analysis of the material with the highest mean reference temperature in a beltline ring forging in the U.S. PWR fleet at the end of an 80-year operating interval.

KEY FINDINGS

- The results from the assessment indicate that the risk associated with the presence of carbon macrosegregation in PWR ring and head forgings is significantly lower than current regulatory risk related criteria.
- Acceptable margins against failure would be maintained even if carbon macrosegregation were to be present in the large forgings used in the primary pressure boundary of PWRs.
- In a number of instances, factors greater than three on the macrosegregation distributions that have actually been measured for ring and head forgings were needed to reach the risk criteria CPF = 1E-6 or 95% TWCF = 1E-6 yr^{-1}. Based on previous extensive work documented in the literature, macrosegregation levels more than three times the measured values are not considered credible.

- The results from this work indicate that there is substantial margin against failure through an 80-year operating interval when conservative distributions of carbon macrosegregation are postulated to be present in the RPV, S/G and pressurizer ring and head forgings in PWRs.

WHY THIS MATTERS

The recent discovery of high carbon levels measured *in situ* on some RPV heads and S/G channel heads has caused long plant outages, costly inspections to address the concerns for integrity, and plant operational restrictions. This research shows that the presence of carbon macrosegregation does not significantly affect pressure boundary integrity.

HOW TO APPLY RESULTS

This research can be referenced to address concerns for carbon macrosegregation.

EPRI CONTACTS: Timothy Hardin, Technical Executive, thardin@epri.com; and Elliot J. Long, Senior Technical Leader, elong@epri.com

PROGRAM: Materials Reliability Program, 41.01.04

IMPLEMENTATION CATEGORY: Reference

CONTENTS

LIST OF FIGURES

LIST OF TABLES

1
INTRODUCTION AND OBJECTIVES

Introduction

Macrosegregation is the segregation of the alloying elements over macroscopic distances in a large ingot. As the molten metal cools and solidifies in the mold, alloying elements (e.g., carbon) that have lower solubility in the solid phase concentrate in the remaining liquid phase. Convective currents carry the carbon-rich liquid towards the top of the ingot, with carbon-depleted solute in the lower part. This process produces large regions of heterogeneity in the ingot. The presence of carbon macrosegregation depends on the ingot pouring, cooling and various other processes that are implemented prior to forging and heat treatment.

These heterogeneous regions can have carbon contents that are either higher or lower than the nominal (average) carbon content in the ingot [1]. Typically, the nominal carbon content in the large forgings used in nuclear reactors ranges from 0.15 wt.% to 0.2 wt.%, while areas of positive carbon segregation can have 0.25 wt.% or more. The material in regions with elevated carbon content can have reduced fracture toughness (the resistance to fracture from flaws that may be present in the material). There are relatively few previous experimental investigations where the change in material fracture toughness has been measured as a function of carbon content. The data that are available indicate that material with elevated carbon content can have lower fracture toughness in both the transition and upper shelf toughness regions [2-6].

Carbon macrosegregation is an important consideration for casting vendors, who may have to reject ingots found to have carbon macrosegregation, and nuclear steam supply system (NSSS) vendors, owners of commercial nuclear power generation facilities and regulatory authorities, who are concerned that carbon macrosegregation may degrade the material resistance to fracture and the structural integrity of large forged pressurized components.

Regions of high carbon macrosegregation have been found or have been identified as having the potential for being present in various large nuclear components in France. The affected components include RPV head forgings, and S/G ring forgings and bottom channel head forgings [4, 5, 7, 8].

The Risk of Component Failure from Macrosegregation in Forgings

Generally, regulatory evaluations of the integrity of the RPV and other pressurized components in nuclear safety systems include the conservative assumption that propagation of a flaw through the vessel wall will produce component failure and potentially lead to reactor core damage. Acceptable margins against failure of pressurized components in nuclear safety systems must be maintained throughout their service life to ensure core integrity for all operational and postulated transient loading events. Should carbon macrosegregation substantially reduce the toughness in safety components then the margins against through-wall flaw propagation may fall below those specified by regulatory requirements to ensure adequate component and reactor core integrity.

Report Objective

The objective of this report is to address the implications of the potential presence of carbon macrosegregation in large forged, PWR pressure retaining components. The specific objective is to assess the structural significance of the presence of carbon macrosegregation in RPV beltline and nozzle shell course ring forgings, RPV head forgings, and S/G and pressurizer ring and head forgings through the end of an 80-year operating interval. This assessment is made using the NRC risk safety criterion: the 95th percentile through-wall cracking frequency (95% TWCF) < 10^{-6} yr^{-1} [9].

Report Scope

Section 2 of this report provides an overview of the casting and forging processes used to produce large forgings in pressurized nuclear components, a brief description of the formation of carbon macrosegregation in large steel castings, and a summary of the experience with carbon macrosegregation that has been found in large structural components in nuclear steam supply systems. Section 3 describes the probabilistic fracture mechanics (PFM) analysis procedure and input that were used to calculate the 95% TWCF and determine the maximum value of carbon macrosegregation for which the 95% TWCF would not exceed 1E-6 yr^{-1} through an 80-year operating interval for ring and head forgings with postulated carbon macrosegregation. Section 4 provides the computational results. A summary of the results and conclusions are presented in Section 5.

2
BACKGROUND

Casting and Forging Processes for Large Pressure Vessel Ring Forgings

Carbon macrosegregation occurs during cooling and solidification of the molten metal in the mold [1]. Ingots weighing up to several hundred tons are used to manufacture forgings used in nuclear reactor pressure retaining components. The potential for carbon macrosegregation in these very large ingots is increased due to the reduced solidification rate in larger ingots. Generally, the casting process used to produce ingots for large forgings is referred to as hot top casting. In this process the molten metal is poured into the top of the mold, which consists of the body (the lower portion of the mold) and the riser (the top of the mold). The usable volume of metal in the ingot solidifies in the body of the mold. The final solidification of the molten metal occurs in the riser whose functions are to provide metal to the body to make up for shrinkage and to provide a receptacle for the high carbon content macrosegregation that occurs as the last of the molten metal solidifies. The typical process used to produce a large cast ingot and the final reactor vessel beltline ring forging is summarized in the remainder of this paragraph.

- Scrap iron is melted in a basic electric furnace.
- The molten metal is placed into a low pressure, inert environment to remove gasses (primarily hydrogen and oxygen); this is generally referred to as vacuum degassing.
- The molten metal then is poured into the top of the mold.
- The molten metal cools and solidifies to form the ingot. During this time regions of macrosegregation form and spread throughout the volume of the casting.
- After solidification, the ingot is removed from the mold, the sides of the ingot are smoothed, and the ends of the ingot are cropped to remove the macrosegregation that is present in these regions.
- The ingot is upset forged along its long axis to increase its diameter.
- If the ingot is to be used for a ring forging, a trepan forging process is used to remove a core of material and produce a hole in the center of the forging; this process removes the macrosegregation that is present in the center of the ingot.
- The forging is then mandrel drawn to increase its length and reduce the wall thickness.
- Finally, the forging is saddle forged, mandrel drawn or ring rolled into its approximate final size and shape.
- The forged ring is then heat treated, rough machined, inspected and final machined.

Segregation in Large Cast Ingot Forgings

Molten metal is homogeneous throughout its volume and the element content everywhere in the molten metal is the same as the overall nominal value in the volume. When molten metal is poured into the mold it begins to solidify. Because impurities (nonmetallic inclusions) and alloying elements generally are less soluble in the solid phase than in the liquid phase, they tend to move from the solid phase into the liquid phase, thereby depleting the impurity and element contents in the solid and enriching the impurity and element contents in the liquid [1]. The segregation of the inclusions and alloying elements in the solid and liquid occurs on the microstructural level and is termed microsegregation. As the cooling and solidification continue, convective flows due to density gradients caused by temperature and composition variations in the liquid, and the migration downward of the higher density of depleted solids spread the depleted and enriched phases over large distances throughout the casting [1]. These extended segregated regions are termed macrosegregation.

In the early stages of this process, the element content of solidified metal is lower than the nominal element content of the molten metal. As the cooling progresses the carbon content in the liquid phase continues to increase, and as the carbon enriched liquid solidifies the carbon content in the solid increases. In the latter stages of cooling the liquid with the highest enrichment solidifies last near the center and top of the ingot, and the latter formed solid phases have element contents that can be substantially higher than the nominal value. At the end of the solidification the average element composition in the ingot is the same as the nominal value in the molten metal; however, the ingot now contains various defects and regions of heterogeneity, where the element contents either can be higher or lower than the nominal values. The regions in the ingot where the element composition is less than the nominal composition are said to have negative macrosegregation and the regions in the ingot where the element composition is greater than the nominal composition are said to have positive macrosegregation [1].

Figure 2-1 illustrates the types and locations of macrosegregation that may be found in large, static cast hot topped steel ingots [1]. Generally, solidification first occurs in the outer and lower portions of the ingot. These regions have element contents that are lower than the nominal values in the ingot and have negative macrosegregation. In the later stages of cooling, solidification occurs in the upper and center regions of the ingot, as illustrated by the “A” and “V” segregates in Figure 2-1. These regions have element contents that are higher than the nominal values in the ingot and have positive macrosegregation. Final cooling and solidification occur in the upper and central portion of the ingot as illustrated by the “V” segregates in Figure 2-1. This region contains the highest level of macrosegregation and can also contain relatively high concentrations of imperfections and impurities, such as shrinkage and nonmetallic inclusions.

If a ring is to be forged, then trepan forging is used to remove a core of material from the center of the forging; this process removes most of the “V” macrosegregation that is present in the center of the forging. Some of the “A” macrosegregation then will remain and extend along the length of the forging both at the surface and embedded in the wall. The portions of the ingot that are discarded and the carbon macrosegregation that is removed by the cropping and trepan forging operations are illustrated in Figure 2-2. If a head is to be forged, then the center is not trepanned, and the “A” and “V” segregates not removed by cropping the top of the ingot will remain in the forged component.

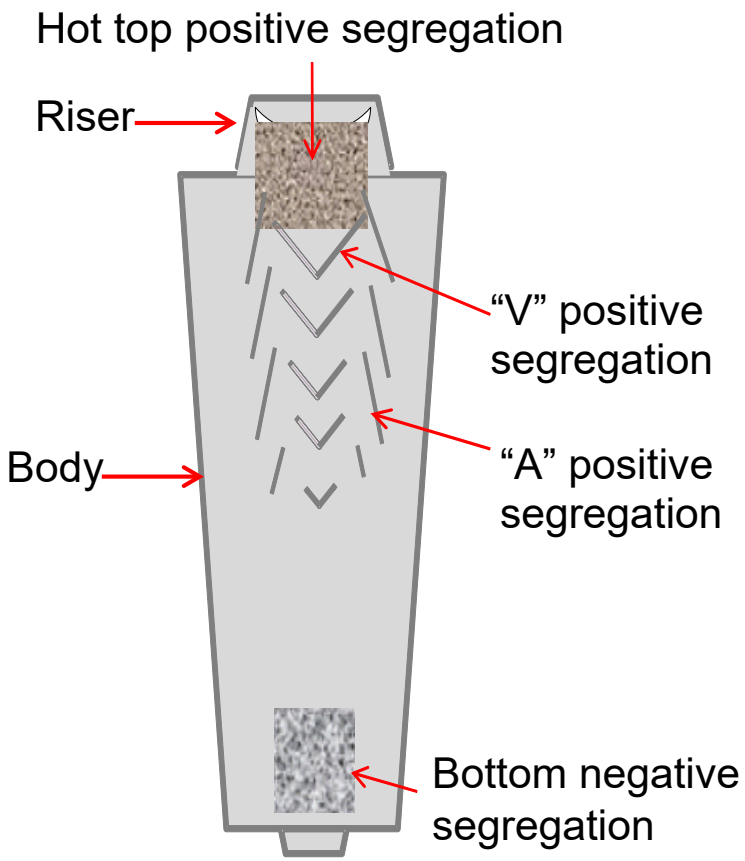

Figure 2-1
Illustration of Classic Macrosegregation Regions in Static Cast Hot Topped Steel Ingots

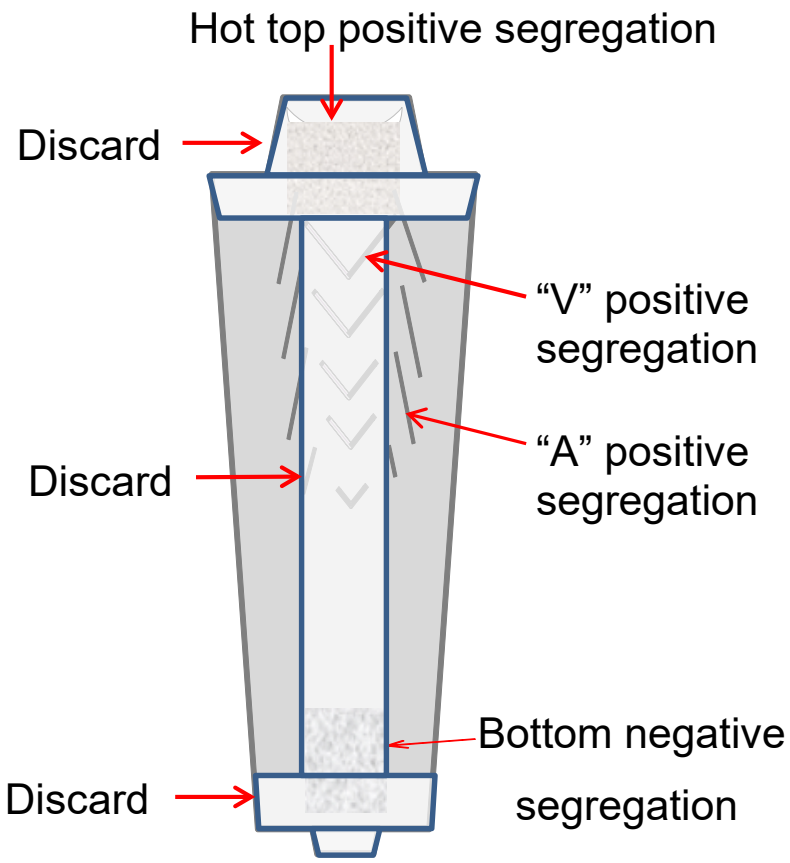

Figure 2-2
Illustration of Discarded Regions of Macrosegregation in Static Cast Hot Topped Steel Ingots used for Ring Forgings

Potential for Carbon Macrosegregation in Nuclear Structural Components

The presence of macrosegregation in large cast steel ingots has been known and studied for some time [1]. Carbon macrosegregation is an important consideration for casting vendors, who may have to reject ingots found to have carbon macrosegregation, and NSSS vendors, owners of commercial nuclear power generation facilities and regulatory authorities, who are concerned that carbon macrosegregation may degrade the material resistance to fracture and the structural integrity of large forged pressurized components [1].

Casting vendors have developed and implemented methods to preclude or retard the formation of carbon macrosegregation in large ingots prior to the solidification of the molten metal [1]. These methods include optimizing the mold design and the composition of certain elements in the steel (e.g., Si and Mn), and implementing beneficial ingot pouring and cooling strategies. Casting vendors often use various algorithms to help optimize the casting process and predict and reduce the potential for carbon macrosegregation [1]. After removing the ingot from the mold, mechanical processes, such as cropping and trepanning are used to remove portions of the remaining macrosegregation from the ingot.

In 2006, the French Nuclear Safety Authority (ASN) introduced new regulations to verify compliance with the fracture toughness requirements for materials in large forged components in

nuclear reactor safety systems [4]. The new regulations specified that the fabricator must consider possible heterogeneity and show how heterogeneous components meet the fracture toughness requirements. However, specific acceptable qualification methods to demonstrate adequate toughness in regions with potential heterogeneities were not specified until 2011.

In 2012, the NSSS vendor AREVA was required to perform qualification tests for the materials in the RPV at the Flamanville 3 (FA3) reactor. However, at the time the qualification tests were to be performed the RPV had already been fabricated and installed. Consequently, the qualification tests were performed using representative materials from RPV top and bottom heads that had been cast and forged using the same procedures used to fabricate the top and bottom heads in the RPV in the FA3 reactor [4]. In 2014, AREVA notified the ASN that the results from some of the qualification tests indicated that the material fracture toughness was less than the regulatory requirement [4].

To determine the cause of the low material fracture toughness AREVA performed a series of measurements to map the carbon content and identify the extent of macrosegregation in the representative head materials [4]. The measurements indicated the presence of positive carbon macrosegregation in the head near the top of the dome [4]. The macrosegregation extended radially over a diameter of about one meter and axially from the outer surface of the dome to a depth of approximately half the wall thickness. The measured carbon content had a maximum value of about 0.3 wt. % near the outer surface of the dome and gradually decreased to the nominal value of about 0.18 wt. % at mid-wall [4]. Based on these measurements AREVA attributed the low fracture toughness to the presence of the carbon macrosegregation [4].

Three vendors have provided large forged NSSS components for French reactors, including Creusot Forge, Japan Casting and Forge Corporation (JCFC) and Japan Steel Works (JSW). The RPV top and bottom head forgings at FA3 were supplied by Creusot Forge.

Based on the results found for the representative materials in the RPV heads at FA3, ASN required AREVA and the French utility, Électricité de France (EDF), to review quality records and manufacturing processes for pressurizer heads and shells, S/G shells, tube sheets and channel heads, and RPV shells and heads in French reactors to determine if these components have the potential for macrosegregation.

The results from that review identified the potential for carbon macrosegregation in the S/G bottom hemispherical channel heads at 18 reactors at 9 sites in France [7]. These channel heads had been provided by either Creusot Forge or JCFC. Of the 18 reactors, 12 had forgings supplied by JCFC that were found to have macrosegregation with particularly high carbon content [7]. The review of the quality records and manufacturing processes indicated that large forged components supplied by Japan Steel Works (JSW) are not susceptible to carbon macrosegregation.

ASN asked EDF to take several actions to justify the acceptability of the forgings identified as susceptible, including: perform non-destructive surface carbon measurements; perform ultrasonic testing (UT) to detect flaws; conduct a structural integrity assessment for susceptibility to brittle fracture; and to adopt certain compensatory operational measures to limit thermal shocks to the channel heads.

When the carbon measurements were performed on the S/G channel heads the maximum carbon content for the S/G bottom channel head forgings supplied by Creusot Forge was reported to be

C = 0.30 wt. % [5], while the maximum carbon content for the S/G bottom channel head forgings supplied by JCFC was reported to be C ≥ 0.39 wt. % [10].

The potential for macrosegregation also was identified in S/G shells at the French reactors Fessenheim-2, Flamanville-3 and Gravelines-5 [8]. The macrosegregation in these S/G shells was present because improper manufacturing or reporting procedures were not revealed during fabrication, and the shells were allowed to be placed in the S/Gs instead of being scrapped [8].

In August 2016, after being briefed by ASN on the experience in France, the Nuclear Regulation Authority, Japan, (NRA) requested that Japanese utilities identify the manufacturers and manufacturing methods of the Class 1 components in PWR reactor pressure vessels, steam generators and pressurizers, and in boiling water reactor (BWR) reactor pressure vessels [11]. The NRA order also required that utilities evaluate any RPV, S/G and pressurizer forgings for the possibility of having a carbon concentration that exceeds the relevant standard (e.g., Japanese Industrial Standards) and report the evaluation to the NRA by October 31, 2016. The results from that survey indicated that forgings are present in the top and bottom heads and ring shell in several BWR reactors and in the top head and ring shell in several PWR reactors. The surveys reported by the utilities identified no forged S/G bottom channel heads or pressurizer bottom heads in Japanese PWRs.

Based on review of the manufacturing processes in Japan, the Japanese utilities have concluded that it is unlikely that the forgings in Japanese reactors contain carbon contents higher than the limits specified in the construction codes. This conclusion is based on the carefully controlled manufacturing methods, quality control, confirmatory testing and documentation associated with the fabrication of large forged NSSS components in Japanese reactors.

Copper and Phosphorus Co-Macrosegregation

Most of the emphasis on macrosegregation in large steel ingots has been focused on carbon. However, it has been reported that when carbon macrosegregation occurs, copper and phosphorus macrosegregation will also occur, and is proportional to the level of carbon macrosegregation [12]. Because copper and phosphorus are known to degrade material fracture toughness when the material is irradiated, increased copper and phosphorous contents due to macrosegregation can further reduce the material fracture toughness due to neutron irradiation during reactor operation. Consequently, evaluation of the effect of macrosegregation on the structural integrity of forgings should include the effect of carbon, copper and phosphorous macrosegregation. The combined effects of carbon, copper and phosphorous macrosegregation on RPV integrity are described in Section 3 and are included in the analysis results presented in Section 4.

3
PFM ANALYSIS APPROACH AND INPUT

Introduction

Macrosegregation in large steel ingots can increase the material carbon, copper and phosphorus contents and reduce the material fracture toughness over extended portions of large, forged structural components in nuclear reactors.

Although macrosegregation has not been identified in large forged components at operating reactors in the U. S., the work described in this chapter was initiated by MRP to demonstrate that acceptable levels of risk are maintained through the end of an 80-year operating interval for PWRs with postulated carbon macrosegregation in large forged, pressure retaining components.

The risk assessment was made by evaluating several forged components and two classes of loading events. The forged components include: a) ring forgings in the RPV beltline and nozzle shell courses, steam generator (S/G) upper and lower shells and the pressurizer shell, and b) solid, one-piece hemispherical forgings in the RPV heads, S/G channel heads and pressurizer heads. The loading events used in the risk evaluation include pressurized thermal shock (PTS) transient events and a normal RPV cooldown event.

The acceptable levels of risk used in this study are defined by: the 95th percentile through-wall cracking frequency (95% TWCF) < 10^{-6} yr^{-1} for PTS events, and the conditional probability of failure (CPF) < 10^{-6} for the normal reactor cooldown event. These risk criteria were selected to maintain consistency with the integrity risk criteria used by the NRC to define the Alternate Fracture Toughness Requirements for Protection Against Thermal Shock Events (Alternate PTS Rule), 10CFR50.61a [9], and other previous work for assessing RPV integrity during normal reactor cooldown [13].

Approach

This effort involved several steps to define and obtain the data and computational tools needed to complete the risk assessment, including:

- Determine the beltline ring forging material with the maximum reference temperature, $RT_{MAX,}$ at the end of the 80-year operating period for the population of U.S. reactor vessels with beltline ring forgings.
- Determine carbon, copper and phosphorus macrosegregation distributions in ring and head forgings fabricated from large conventional ingots.
- Construct models of ring and head forgings, which include applicable welds, fluence levels and carbon, copper and phosphorus macrosegregation distributions.
- Apply the embedded and surface flaw distributions previously used by the NRC to define the Alternate PTS Rule, 10CFR50.61a [14-16].

- Apply the population of postulated transient events and associated event frequencies that were previously used by the NRC to define the Alternate PTS Rule, 10CFR50.61a [14-16].
- Apply the pressure and temperature time histories for a normal RPV cooldown along the Appendix G allowable pressure temperature (P-T) limit curve [17].
- Perform PFM analyses to determine the CPF and 95% TWCF over a wide range of carbon macrosegregation levels to demonstrate compliance with the risk criteria through an 80-year operating interval for large forged, pressure retaining components postulated to have carbon macrosegregation.
- Perform a sensitivity study to determine the effect of vessel wall thickness on the calculated CPF and 95% TWCF for the range of wall thicknesses in PWR head and ring forgings.
- Perform the PFM analyses to maintain consistency with the methodology previously used by the NRC to define the Alternate PTS Rule, 10CFR50.61a [14-16] using the latest publicly released NRC software, FAVOR v16.1 [18].
- Because postulated, rather than actual, macrosegregation distributions are being evaluated, account for variable uncertainties where appropriate.

Analysis Input

Forged Component Dimensions and Material Properties

A previous evaluation of the population of U.S. reactor vessels with beltline ring forgings identified the RPV beltline forging material with the highest value of reference temperature, RT_{MAX}, at a 60-year operating interval [19]. This same material was used in this study, where the fluence values at an 80-year operating interval were obtained by linear extrapolation of the fluence values reported for a 60-year operating interval.

The forged components evaluated in the PFM analyses include the RPV beltline, nozzle shell course and closure and bottom heads, the steam generator (S/G) channel head and upper and lower shells, and the pressurizer shell and heads. The forged components and their dimensions are listed in Table 3-1 along with the peak fluence at the component inner surface at the end of an 80-year operating interval.

The PFM analyses were performed for both a thick wall (8.45-inch) (215-mm) RPV and a thin wall (6.7-inch) (170-mm) RPV to encompass the applicable range of wall thicknesses in PWR RPV beltline ring forgings. The cladding thickness on the inner surface of each component listed in Table 3-1 is 0.16-inch (4-mm), except for the S/G upper and lower shells, which are not exposed to the primary coolant and are not clad.

Table 3-1
Forged Components, Dimensions and Peak ID Fluence Evaluated in the Risk Analyses

Forged Component	Inner Radius to the Clad-Base Metal Interface (CBMI)	Base Metal Wall Thickness	R/t	Total Shell Height	Peak ID Fluence at 80 years
	inch	inch	-	inch	n/cm^2
Thick wall RPV: beltline	85.6	8.45	10.1	144	3.67E19
Thick wall RPV: nozzle shell course	85.6	10.8	7.9	96	4.95E16
Thick wall RPV: heads	85.6	7.0	12.8	85.6	3.44E15
Thin wall RPV: beltline	66.2	6.7	9.9	144	3.67E19
Thin wall RPV: nozzle shell course	66.2	9.0	7.4	96	4.95E16
Thin wall RPV: heads	66.2	5.4	12.3	66	3.44E15
S/G upper shell	80.0	3.5	22.9	200	3.44E15
S/G lower shell	60.0	2.6	23.1	244	3.44E15
S/G channel head	59.5	9.63	6.2	59.5	3.44E15
Pressurizer shell	44.2	5.0	8.8	590	3.44E15
Pressurizer heads	44.2	4.0	11.1	44.2	3.44E15

The nominal values of carbon content, initial RT_{NDT}, and the irradiation degradation related variables (Cu, Ni, Mn, P) used in the PFM and risk analyses for each of the components listed in Table 3-1 are summarized in Table 3-2 [19].

Table 3-2
Forging Material Variable Values used in the Risk Analyses

Variable	Value
Nominal reported carbon content, C_o, wt. %	0.17
Nominal reported copper content, Cu_o, wt. %	0.13
Nominal reported nickel content, Ni_o, wt. %	0.76
Nominal reported phosphorus content, P_o, wt. %	0.015
Nominal reported manganese content, Mn_o, wt. %	0.62
Nominal reported initial RT_{NDT}, $RT_{NDT(Uo)}$, °F	73

Element Macrosegregation Metrics

Carbon macrosegregation often is characterized by the metric,

$\Delta C/C_o$, where: Eq. 3-1

$\Delta C = (C - C_o)$,

C is the carbon content in the macrosegregation region, and

C_o is the nominal or average carbon content in the ingot.

For computational convenience, the carbon content in the macrosegregation region can be described in terms of the carbon macrosegregation. Using Eq. 3-1 the carbon content in the macrosegregation region can be expressed as:

$$C = C_o \bullet [1 + (\Delta C/C_o)]. \quad \text{Eq. 3-2}$$

When carbon macrosegregation occurs in large forgings it is accompanied by copper and phosphorus macrosegregation. The percent copper macrosegregation is reported to be 40% of the percent positive carbon macrosegregation [12]. Using Eq. 3-2 the copper content in the macrosegregation region, Cu, can be determined as a function of the carbon macrosegregation and can be expressed as:

$$Cu = Cu_o \bullet [1 + 0.4 \bullet (\Delta C/C_o)], \text{ where} \quad \text{Eq. 3-3}$$

Cu_o is the nominal or average copper content in the ingot.

The percent phosphorus macrosegregation is reported to be 70% of the percent positive carbon macrosegregation [12]. Using Eq. 3-2 the phosphorus content in the macrosegregation region, P, can be determined as a function of the carbon macrosegregation and can be expressed as:

$$P = P_o \bullet [1 + 0.7 \bullet (\Delta C/C_o)], \text{ where} \quad \text{Eq. 3-4}$$

P_o is the nominal or average phosphorous content in the ingot.

Figure 3-1 shows a plot of the carbon, copper and phosphorus contents in a macrosegregation region as a function of the percent carbon macrosegregation for the nominal element contents C_o = 0.17 wt.%, Cu_o = 0.13 wt.% and P_o = 0.015 wt.% listed in Table 3-2.

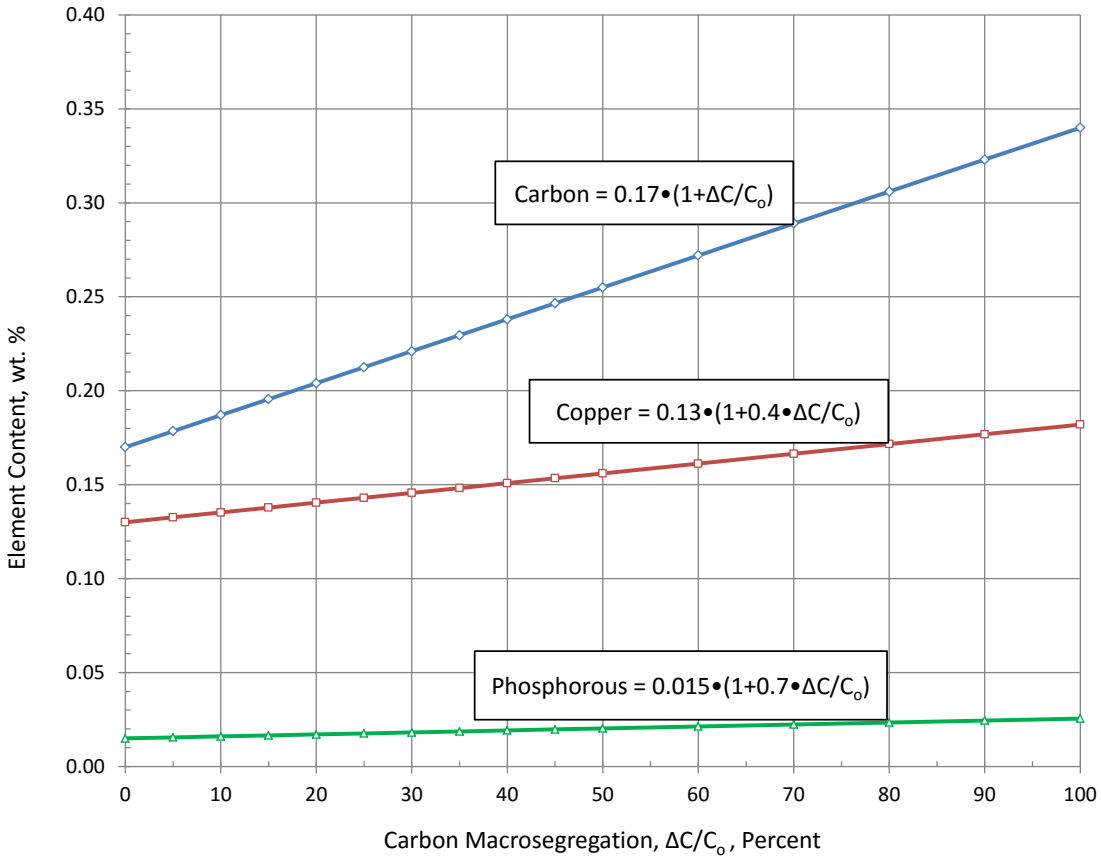

Figure 3-1
Carbon, Copper and Phosphorus Contents as a Function of Percent Carbon Macrosegregation

Carbon Macrosegregation and Fracture Toughness Metrics

The fracture toughness of ferritic steels in a macrosegregation region is determined by and is inversely proportional to the reference temperature in the macrosegregation region, RT_{MAX}, or

$$RT_{MAX} = RT_{NDT(U)} + \Delta T_{30}, \text{ where,} \qquad \text{Eq. 3-5}$$

$RT_{NDT(U)}$ is the unirradiated component of the reference temperature in the macrosegregation region, and

ΔT_{30} is the change in the reference temperature in a macrosegregation region from neutron irradiation and is computed using the fluence at the CBMI from the relationship specified in the Alternate PTS Rule, 10CFR50.61a [9].

Initial RT_{NDT} in the Macrosegregation Region

The elevated carbon content in the macrosegregation regions will increase the initial RT_{NDT} in the macrosegregation region. The initial R_{TNDT} in the macrosegregation region, $RT_{NDT(U)}$, is expressed as:

$$RT_{NDT(U)} = RT_{NDT(Uo)} + K \bullet \Delta C, \text{ where} \qquad \text{Eq. 3-6}$$

$RT_{NDT(Uo)}$ is the unirradiated reference temperature (initial RT_{NDT}), and is defined in Paragraph NB-2331 of Section III of the ASME Code [20] or by other procedures acceptable to regulatory authorities [21], and

K is the change in $RT_{NDT(U)}$ as a function the change in carbon content, °F/wt. % C, and is determined from experimental data. Information from several sources [2-6] was used to correlate the change in $RT_{NDT(U)}$ with the change in carbon content and determine K for the forging material; the results are summarized in Table 3-3.

Table 3-3
Summary of Data used to Calculate the Change in Temperature per Unit Change in Carbon Content

Temperature Interval, ΔT	Carbon Interval, ΔC	K = ΔT/ΔC	K	Reference
°C	wt.%	°C/wt.%C	°F/wt.%C	
93	0.30	310.0	558	2
30.7	0.10	307.0	552	3
30	0.11	272.7	491	4,5
30	0.10	300.0	540	4,5
35	0.11	318.2	573	4,5
35	0.10	350.0	630	4,5
73	0.23	317.4	571	6

Reference [2] contains a plot of the 50% shear transition temperature as a function of carbon content over a range from carbon = 0.1 wt.% to 0.8 wt.%. A linear fit of these data in the range from carbon = 0.1 wt.% to 0.4 wt.% indicates that ΔT = 93°C and, consequently, K = 558 °F/wt.% C. Reference [3] provides a plot of the ductile brittle transition temperature as a function of carbon content over a range from carbon = 0.08 wt.% to 0.18 wt.%. A linear fit of these data indicates that ΔT = 30.7 °C and, consequently, K = 552 °F/wt.% C. In References [4, 5] the temperature increase that would be required to increase the average Charpy energy measured at 0°C to the value required by French specifications was estimated for specimens with carbon content in the range from 0.28 wt.% to 0.29 wt.% [4,5]. This temperature increase was estimated to be in the range from 30°C to 35°C [4]. These results indicate that K would be in the range from about 491°F/wt.% C to 630°F/wt.% C for the measured nominal carbon content C_o = 0.18 wt.%. Information in Reference [6] indicates that there was an increase in the transition temperature of 73°C when the carbon content was increased from 0.17 wt. % to 0.4 wt.%, or K = 571 °F/wt.% C.

The average of the values listed in Table 3-3 is approximately K = 560 °F/wt.% C, and is used to calculate the adjusted $RT_{NDT(U)}$ from Eq. 3-6, or

$RT_{NDT(U)} = RT_{NDT(Uo)} + 560 \bullet \Delta C$, °F.

Because carbon macrosegregation often is expressed as percent macrosegregation it is convenient to express $RT_{NDT(U)}$ as a function of the fractional form of percent carbon macrosegregation, $(\Delta C/\Delta C_o)$, or

$$RT_{NDT(U)} = RT_{NDT(Uo)} + C_o \bullet 560 \bullet (\Delta C/C_o). \quad \text{Eq. 3-7}$$

The input to the FAVOR software includes the standard deviation for $RT_{NDT(U)}$, σ_U, which can be expressed for this evaluation as:

$$\sigma_U = (\sigma_i^2 + \sigma_k^2)^{0.5}, \text{ where} \quad \text{Eq. 3-8}$$

σ_i and σ_k are the standard deviations for the temperatures $RT_{NDT(Uo)}$ and $C_o \bullet 560 \bullet (\Delta C/C_o)$, respectively, in Eq. 3-7. The value of σ_i is determined using the guidelines in [22]. Because the value of $RT_{NDT(Uo)}$ listed in Table 3-2 was determined by actual measurement of archival plant specific vessel material [19], σ_i can be set equal to zero [22], and then $\sigma_U = \sigma_k$. Since σ_k arises from the uncertainty in the value of K, and because the standard deviation input into FAVOR is a temperature, then σ_k must be a temperature and is determined by the product of the standard deviation for K and the value of ΔC for a specified macrosegregation level. Using the data in Table 3-3, the standard deviation for K is 41.7 °F/wt.%C, and σ_k is the product, 41.7 • ΔC, or using the form of Eq. 3-7

$$\sigma_U = \sigma_k = 41.7 \bullet C_o \bullet (\Delta C/C_o), \text{ °F}. \quad \text{Eq. 3-9}$$

The value of σ_k in Eq. 3-9 is a variable and is a function of the macrosegregation level, $(\Delta C/C_o)$. For example, if there is no macrosegregation then $(\Delta C/C_o) = 0$, and $\sigma_U = 0$. Similarly, if the percent carbon macrosegregation level is 75% and $C_o = 0.17$ wt.%, then the standard deviation for a region with 75% macrosegregation is $\sigma_U = (41.7°F/wt.\%C) \bullet (0.17 \text{ wt.}\%C) \bullet 0.75 = 5.32°F$ (2.96°C).

ΔT_{30} in the Macrosegregation Region

When carbon macrosegregation occurs in large forgings it is accompanied by copper and phosphorus macrosegregation with increased copper and phosphorous contents as indicated in Eq. 3-3 and Eq. 3-4 and Figure 3-1. The elevated copper and phosphorus contents are used to calculate ΔT_{30} and will increase the value of ΔT_{30} in the macrosegregation region.

RT_{MAX} in the Macrosegregation Region

The relationship for the reference temperature that includes the effect of carbon macrosegregation and the accompanying copper and phosphorus co-segregation is obtained by substituting Eq. 3-7 into Eq. 3-5, or

$$RT_{MAX} = RT_{NDT(Uo)} + C_o \bullet 560 \bullet (\Delta C/C_o) + \Delta T_{30}, \text{ °F}. \quad \text{Eq. 3-10}$$

Figure 3-2 shows a plot of the $RT_{NDT(U)}$, shift in RT_{NDT} (ΔT_{30}) and RT_{MAX}, in the macrosegregation region as a function of the percent carbon macrosegregation for the nominal values of $RT_{NDT(Uo)} = 73°F$ (23°C), $C_o = 0.17$ wt.%, $Cu_o = 0.13$ wt.% and $P_o = 0.015$ wt.% listed in Table 3-2. The values of ΔT_{30} were calculated from the relationship specified in Reference [9] using the RPV beltline surface fluence = 3.67E19 n/cm^2 and the Cu and P contents calculated from Eq. 3-3 and Eq. 3-4.

In the low fluence regions, ΔT_{30} is less than 10°F (5.56°C) at macrosegregation levels up to 300%, and RT_{MAX} is essentially equal to $RT_{NDT(U)}$, over a wide range of carbon macrosegregation levels.

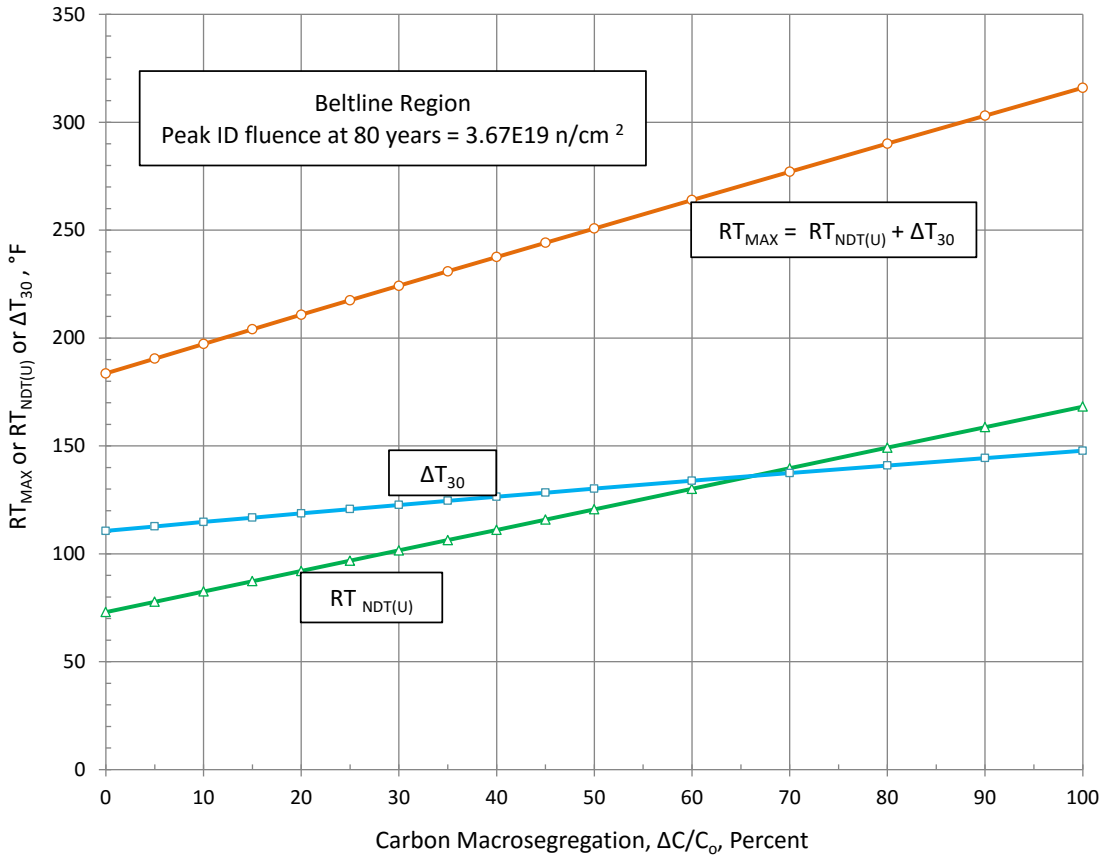

Figure 3-2
Initial RT_{NDT}, Shift in RT_{NDT} and Reference Temperature RT_{MAX} as a Function of Percent Carbon Macrosegregation

Carbon Macrosegregation Distributions

Computation of the CPF and 95% TWCF for forgings with carbon macrosegregation requires the definition of the distribution of positive macrosegregation in the forging. Distributions of carbon macrosegregation have been measured previously for both ring forgings [12] and head forgings [5]. These distributions are reported either as carbon content or percent carbon macrosegregation.

Carbon Macrosegregation Distribution in Ring Forgings

A quantitative mapping of positive macrosegregation in a large nozzle shell course ring forging is described in Reference [12] and is used in this work to calculate the CPF and 95% TWCF for large ring forgings. The information in Reference [12] indicates the overall length of the shell course is approximately 108-inches (2743-mm). Starting at the top, the first 54-inches (1372-mm) of the shell has percent carbon macrosegregation ranging from 6 percent to 12 percent in

the inner quarter of the shell wall thickness. The next 11-inches (279-mm) have no positive carbon macrosegregation. The remaining 43-inches (1092-mm) of the shell course have percent carbon macrosegregation ranging from negative 25 percent to positive 25 percent. The percent carbon macrosegregation for the 54-inch (1372-mm) and 11-inch (279-mm) shell segments are described semi-quantitatively by color coding (Figure 10 of Reference [12]), while detailed percent carbon macrosegregation measurements are presented for the 43-inch (1092-mm) segment (Figure 14 of Reference [12]).

Table 3-4 summarizes the distribution of positive macrosegregation obtained from Reference [12] in the inner quarter of the vessel wall for the shell segments along the length of the shell course. The first column in Table 3-4 presents the range of measured carbon macrosegregation values in 5 percent intervals. The second column in Table 3-4 lists the number of measured values in each macrosegregation range in the 43-inch (1092-mm) segment at the bottom of the forging, while the third column shows the number of data points in each range as a fraction of the total number of data points for the 43-inch (1092-mm) segment. The values in Column 4 are the product of the length of the shell containing the macrosegregation (43-inches) (1092-mm) and the fraction of the total number of measured values in Column 3; these products represent the heights of the shell segments and their associated levels of macrosegregation in the 43-inch (1092-mm) segment at the bottom of the forging. The fifth column in Table 3-4 is the sum of all the segment lengths for the total 108-inch (2743-mm) shell course length, including the 54-inch (1372-mm) segment length with 6 percent to 12 percent carbon macrosegregation (added proportionally to the $0.05 < \Delta C/C_o \leq 0.10$ and $0.10 < \Delta C/C_o \leq 0.15$ intervals), and the 11-inch (279-mm) segment length with no carbon macrosegregation (added to the $\Delta C/C_o \leq 0$ interval).

Table 3-4
Carbon Macrosegregation Mapping from a Large Nozzle Shell Course Ring Forging

Macrosegregation Interval, $\Delta C / C_o$	No. of Measured Values in 43-inches	Fraction of the Total No. of Measured Values in 43-inches	Segment Lengths in 43-inches	Total Segment Lengths in 108-inches
n/a	n/a	n/a	inch	inch
$\Delta C/C_o \leq 0$	6	0.095	4.1	15.1
$0 < \Delta C/C_o \leq 0.05$	16	0.254	10.92	10.92
$0.05 < \Delta C/C_o \leq 0.10$	11	0.175	7.51	46.08
$0.10 < \Delta C/C_o \leq 0.15$	9	0.143	6.14	21.57
$0.15 < \Delta C/C_o \leq 0.20$	12	0.190	8.19	8.19
$0.20 < \Delta C/C_o < 0.25$	9	0.143	6.14	6.14

Table 3-5 is the carbon macrosegregation distribution used for the PFM analysis of the ring forgings. The first column in Table 3-5 contains a letter to identify the color-coded shell segment and the macrosegregation interval. The second column is the carbon macrosegregation level in the segment and is conservatively defined as the value at the top of the bins shown in Table 3-4. Column 3 is the height of the segment as a fraction of the total height of the ring forging (the values in the last column in Table 3-4 divided by 108-inch (2743-mm), rounded to two decimal

places). The carbon macrosegregation distribution for any ring forging can be defined by multiplying the values in the third column in Table 3-5 by the total height of the ring forging.

Table 3-5
Carbon Macrosegregation Distribution Used in the PFM Analysis of Ring Forgings

Macrosegregation Distribution - Ring Forgings		
Segment Macrosegregation		Segment Height
	$\Delta C/C_o$	Fraction of Total Shell Height
A:	0.0	0.14
B:	0.05	0.10
C:	0.10	0.42
D:	0.15	0.20
E:	0.20	0.08
F:	0.25	0.06

Carbon Macrosegregation Distribution in Head Forgings

A quantitative mapping of positive macrosegregation in several large head forgings is described in Reference [5]. These mappings were used in this work to determine the carbon macrosegregation distribution and calculate the CPF and 95% TWCF for large head forgings. The carbon macrosegregation zone was determined from a series of measured values of carbon content and was found to extend radially about 50-inches (1270-mm) from the center of the dome and more than half way through the thickness [5]. The maximum carbon content in the head forging is located near the outer surface at the center of the dome and is 0.3 wt.%. However, the maximum known measured carbon content in a large head forging is about 0.4 wt.% [10]. To define a carbon macrosegregation distribution that encompasses the known measured data for large head forgings the mapping from [5] was scaled up to be consistent with the maximum reported carbon content in [10].

The macrosegregation mapping in [5] was taken from a forging (upper dome "UA") representative of the forging process used to fabricate the FA3 head forging. Consequently, the FA3 head forging described in [4] and illustrated in Figure 3-3 was used as representative head geometry to define a carbon macrosegregation distribution in large head forgings. The FA3 head forging has a bend radius of 106-inches (2692-mm) and a height of 45.6-inches (1158-mm) from the bottom inside surface of the dome [5]. The macrosegregation region has a diameter of approximately 100-inches (2540-mm) [5]. Using these dimensions, the maximum radius of the forging is 87.1-inches (2212-mm) and the height of the macrosegregation region from the bottom inside surface of the dome is 12.5-inches (318-mm). Consequently, the macrosegregation region covers about 27.5% of the inside surface area of the head, and the remaining 72.5% of the inside area of the head has no macrosegregation.

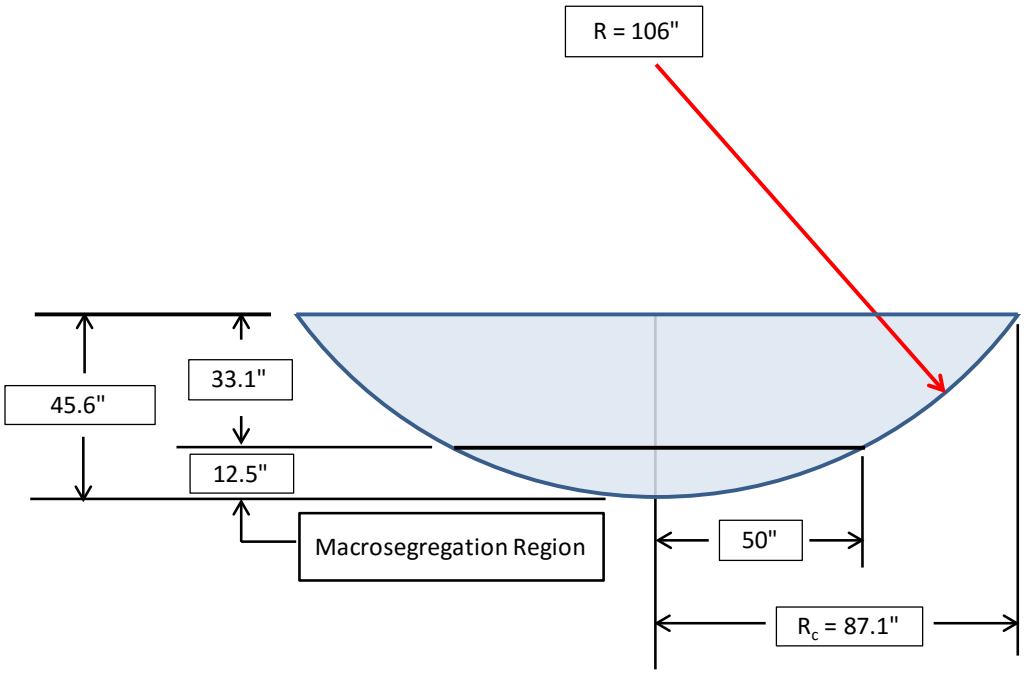

Figure 3-3
Illustration of the Head Forging and Macrosegregation Region

The results from the carbon mapping are presented in Table 3-6 for the macrosegregation region in the outer quarter of the head wall. The first column in Table 3-6 presents the range of measured carbon macrosegregation in 20 percent intervals. There are 100 measured data points in the macrosegregation region in the outer quarter of the head wall, and the second column in Table 3-6 lists the number of measured values [5] in each macrosegregation interval. The third column shows the number of data points in each macrosegregation interval as a fraction of the total number of measured data points in the 12.5-inch (318-mm) high macrosegregation region. The values in Column 4 are the product of the height of the head containing the macrosegregation (12.5-inches) (318-mm) and the fraction of the total number of measured values in Column 3; these products represent the heights of the head segments and their associated levels of macrosegregation in the macrosegregation region. The fifth column in Table 3-6 lists the segment heights and their associated macrosegregation intervals in the total 45.6-inch (1158-mm) head height from the bottom inside surface of the dome to the top of the forging.

Table 3-6
Carbon Macrosegregation Mapping from a Large Head Forging

Macrosegregation Interval, $\Delta C / C_o$	No. of Measured Values in the Macrosegregation Region	Fraction of the Total No. of Measured Values	Segment Height in 12.5-inches	Segment Height in 45.6-inches
n/a	n/a	n/a	inch	inch
$\Delta C/C_o \leq 0$	0	0.0	0.0	33.1
$0 < \Delta C/C_o \leq 0.20$	6	0.06	0.75	0.75
$0.20 < \Delta C/C_o \leq 0.40$	26	0.26	3.26	3.26
$0.40 < \Delta C/C_o \leq 0.60$	24	0.24	3.01	3.01
$0.60 < \Delta C/C_o \leq 0.80$	26	0.26	3.26	3.26
$0.80 < \Delta C/C_o < 1.00$	18	0.18	2.26	2.26

Table 3-7 is the carbon macrosegregation distribution used for the PFM analysis of the head forgings. The first column in Table 3-7 contains a letter to identify the color-coded head segment height and the macrosegregation level. The second column is the level of carbon macrosegregation in the segment and is conservatively defined as the value at the top of the bins shown in Table 3-6. Column 3 is the height of the segment as a fraction of the total height of the head forging (the values in the last column in Table 3-6 divided by 45.6-inches (1158-mm), rounded to two decimal places). The carbon macrosegregation distribution for any head forging can be defined by multiplying the values in the third column in Table 3-7 by the total height of the head forging.

Figure 3-4 is a visual image of the carbon macrosegregation distribution shown in Table 3-7, where the level of macrosegregation diminishes from the red region immediately surrounding the center of the dome, which has the highest macrosegregation level ($0.80 < \Delta C/C_o < 1.00$) and covers 5% of the head surface area, to the light green region, which covers 72% of the head surface area and has no macrosegregation ($\Delta C/C_o \leq 0$).

Table 3-7
Carbon Macrosegregation Distribution used in the PFM Analysis of Head Forgings

Macrosegregation Distribution - Head Forging		
Segment Macrosegregation		Segment Height
	ΔC/Co	Fraction of Total Head Height
A:	0.0	0.72
B:	0.2	0.02
C:	0.4	0.07
D:	0.6	0.07
E:	0.8	0.07
F:	1.0	0.05

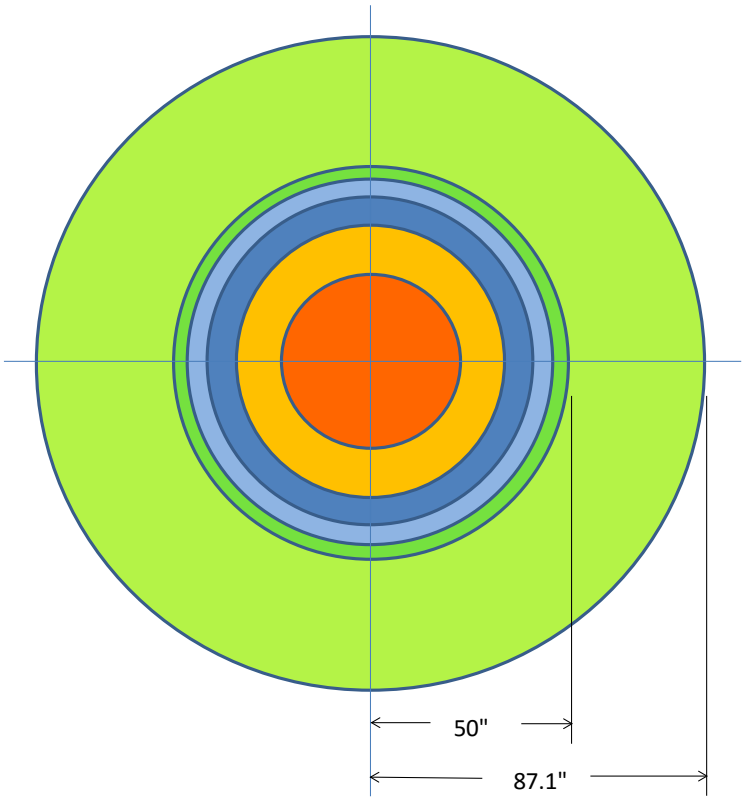

Figure 3-4
Illustration of the Carbon Macrosegregation Distribution Intervals in a Forged Head

Macrosegregation Distributions in FAVOR Models

FAVOR Ring Forging Models

Models containing macrosegregation distributions were constructed for each forged component evaluated with the FAVOR software. Figure 3-5 illustrates the distributions used for the ring forgings. The RPV beltline model includes two shell ring forgings joined by a circumferential weld (which is the typical configuration for a forged-ring vessel) and 12 forged beltline shell segments (six on either side of the weld), each of which has length and a level of macrosegregation indicated by the table at the right of the figure. The shell segments attached to the circumferential weld (Segments F) have the highest level of macrosegregation and the maximum RT_{MAX} in the beltline region; the remaining segments have decreasing values of macrosegregation and RT_{MAX} as the segments are located farther away from the weld. The segments farthest from the weld (Segments A) have no positive macrosegregation. The height of each macrosegregation segment is the product of the total height of the ring forging and the fraction of the total height for the segment listed in the last column in the table in Figure 3-5. For example, if the total height of each RPV beltline ring forging is 72-inches (1829-mm), then the height of the shell segment with 25% carbon macrosegregation (Segment F) is 6 percent of 72-inches (1829-mm), or about 4.3-inches (109-mm) in each beltline shell ring forging.

The RPV nozzle shell course model shown in Figure 3-5 includes a circumferential weld and seven forged beltline shell segments. Again, shell Segment F is attached to the weld and the remaining segments have decreasing values of macrosegregation and RT_{MAX} as the segments are located farther away from the weld. Segment A at the top of the weld attachment is a modeling convenience and has negligible height.

Any number of shell segments in any order and with any axial height can be used to describe the macrosegregation distribution in a ring forging, provided they are consistent with the distribution shown in the table at the right of Figure 3-5. In the configurations shown in Figure 3-5, the forging segment with the highest level of macrosegregation is attached to the weld; this configuration is conservative because the flaws are located in the weld fusion zone, which is adjacent to the region with the highest RT_{MAX} (lowest toughness) and highest stress (thermal gradient, pressure, cladding and weld residual stresses).

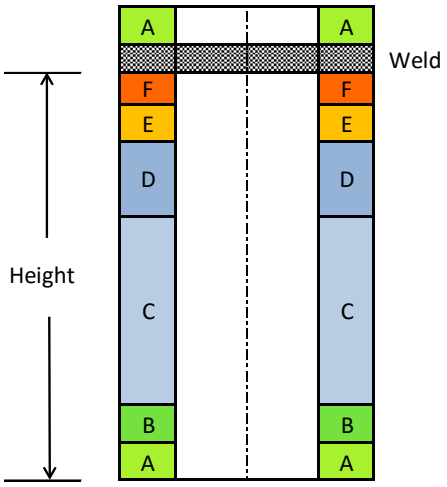

RPV Nozzle Shell Course Ring Forgings

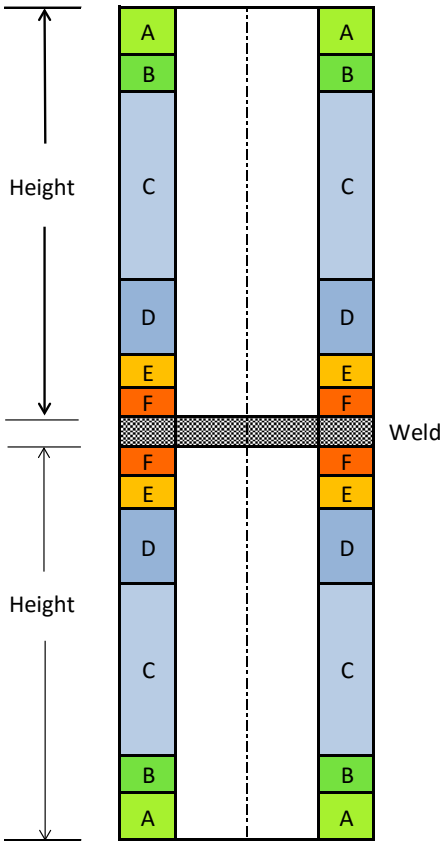

Macrosegregation Distribution - Ring Forgings		
Segment Macrosegregation		Segment Height
	$\Delta C/C_o$ Intervals	Fraction of Total Shell Height
A:	0.00	0.14
B:	0.05	0.10
C:	0.10	0.42
D:	0.15	0.20
E:	0.20	0.08
F:	0.25	0.06

RPV and Pressurizer Ring Forgings

Figure 3-5
Illustration of the FAVOR Models Used to Simulate the Carbon Macrosegregation Distribution for the PFM Analyses of the Ring Forgings

FAVOR Head Forging Models

FAVOR is designed to analyze flaws in cylinders, which contain circumferential surface flaws and embedded axial and circumferential flaws. FAVOR can be used to evaluate vessel heads provided the head is hemispherical; that is, the height and bend radius of the head must be approximately equal to the radius of the attached cylindrical shell. Under these circumstances, the pressure stress in the hemispherical head is the same as the axial pressure stress in a cylinder, and due to symmetry, the stress is the same everywhere in the hemispherical head. Consequently, because the surface flaw distributions in FAVOR contain only circumferential surface flaws, the FAVOR results for evaluation of surface flaws will be directly applicable for hemispherical heads. However, the FAVOR embedded flaw distributions contain both circumferential and axial embedded flaws. In this instance, the FAVOR computational results for the pressure stress and associated pressure K_I component for cylinders may be conservative when used for hemispherical heads.

The FAVOR input for cylinders includes the thickness, radius and height of the cylindrical shell segments. When FAVOR is used to evaluate the hemispherical head, the FAVOR input for head thickness and radius are the thickness and radius of the hemispherical head and the segment heights are the products of the total height of the hemispherical head and the fractional values in the third column of Table 3-7 in each macrosegregation interval.

Figure 3-6 illustrates the carbon macrosegregation distribution used in the FAVOR models for head forgings. There are no welds or penetrations in the high macrosegregation region near the top of the dome in the RPV bottom head or the S/G channel head, and the weld in the FAVOR model is located outside the macrosegregation region. There are penetrations and welds near the top of the dome in the pressurizer heads and the RPV closure head, and the weld in the FAVOR model is placed in the high macrosegregation region.

The macrosegregation distribution for the two FAVOR head models is presented in the table at the right in Figure 3-6. The carbon macrosegregation distribution can be defined for any head forging by multiplying the values in the third column in the table in Figure 3-6 by the height of the hemispherical head forging.

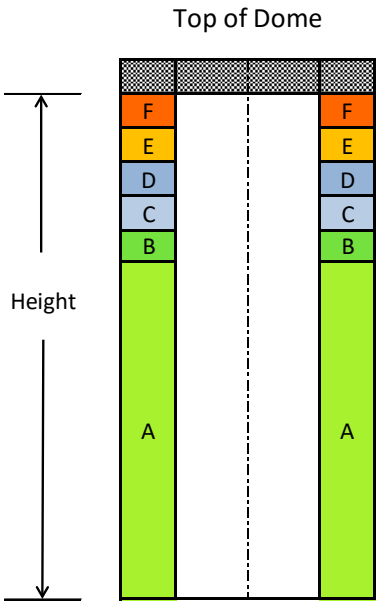

Macrosegregation Distribution - Head Forgings		
	Segment Macrosegregation	Segment Height
	ΔC/Co Intervals	Fraction of Total Head Height
A:	0.0	0.72
B:	0.2	0.02
C:	0.4	0.07
D:	0.6	0.07
E:	0.8	0.07
F:	1.0	0.05

Figure 3-6
Illustration of the FAVOR Models Used to Simulate the Carbon Macrosegregation Distribution for the PFM Analyses of Head Forgings

Other than property changes due to fluence, there is no through-wall variation in material properties or macrosegregation level in the weld or head or ring forging segments; this is a conservative assumption that precludes concerns about non-conservatisms associated with the uncertainty in through-wall properties due to elevated carbon content.

Loading Events

Normal Reactor Cooldown

The cooldown event used in the PFM analyses is a normal RPV cooldown from normal full power operation to cold shutdown. The cooldown was defined as cooldown from 547°F (286°C) to 300°F (149°C) at 100°F /hr. (56°C/hr.), then 300°F (149°C) to 60°F (16°C) at 50°F/hr. (28°C/hr.). This cooldown simulates an initial rapid cooldown rate where heat is extracted using the steam generator from 547°F (286°C) to 300°F (149°C) followed by a lower cooldown rate from 300°F (149°C) to 60°F (16°C) using decay heat removal systems.

The Appendix G allowable P-T limit curves for the cooldown event [17] are presented in Figure 3-7 for vessels with beltline wall thickness of 8.45-inches (215-mm) and 6.7-inches (170-mm). The adjusted reference temperature (ART) values indicated in Figure 3-7 were determined using the procedures in Reference [22] and differ slightly due to the small difference in fluence at the quarter thickness location in the vessel walls. The RPV beltline conditions in both the thick and thin wall vessels listed in Table 3-1 and Table 3-2 were used to define the limiting allowable P-T limit curves shown in Figure 3-7.

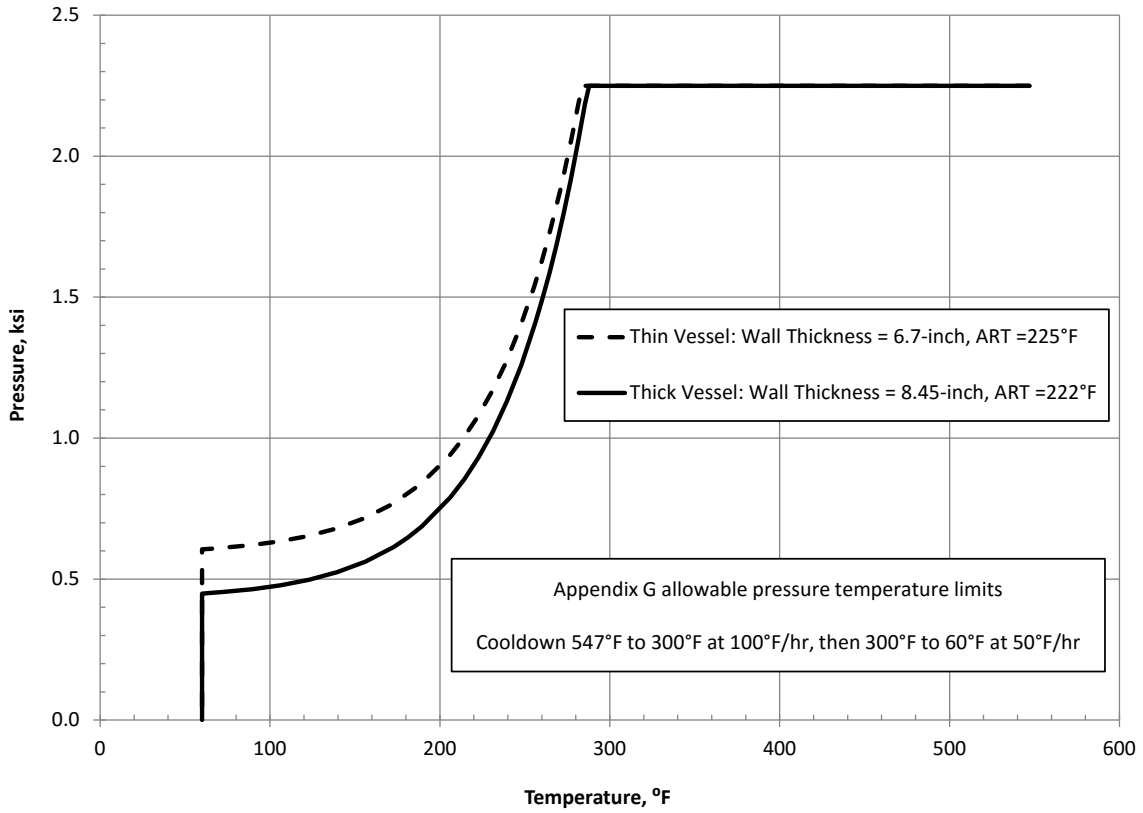

Figure 3-7
Appendix G Allowable RPV Cooldown P-T Limits for the Limiting PWR Beltline Ring Forging Material

The P-T limits shown in Figure 3-7 were used to determine the pressure and temperature time histories that were input into the FAVOR software. The time histories for each of the two RPV wall thicknesses are shown in Figure 3-8. The time histories shown in Figure 3-8 were used to evaluate all the components included in the risk analyses in this study.

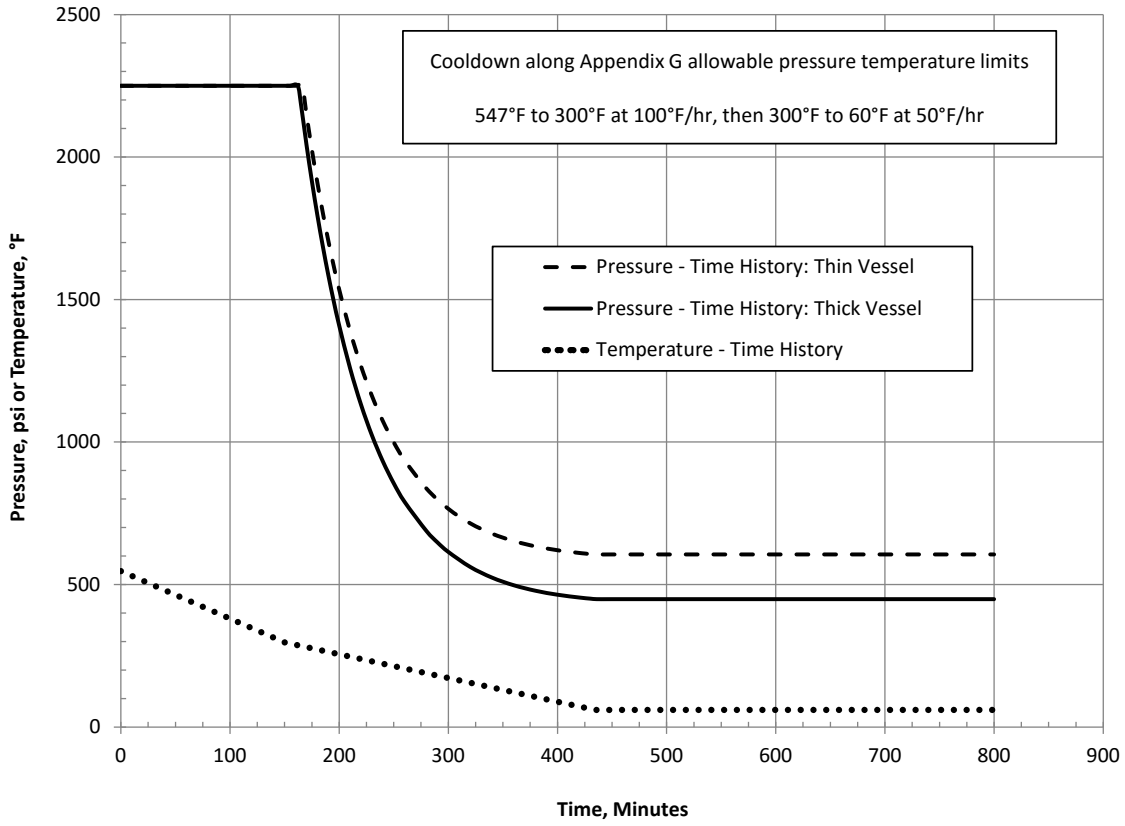

Figure 3-8
RPV Cooldown Pressure and Temperature Time Histories for the Limiting PWR Beltline Ring Forging Material

PTS Transient Events

Because both the thick and thin wall vessels and the beltline ring forging with the highest RT_{MAX} are in reactors of the Westinghouse design, the postulated transient events used in this evaluation are the 61 postulated events used in the NRC PTS evaluation of the Westinghouse-design plant [15]. These transients define the temperature, pressure, and heat transfer coefficient time histories and transient frequency distributions for the events previously determined by the NRC to be potential contributors to TWCF for postulated PTS events at Westinghouse-design plants generally [15]. The initiating events for these transients typically are in one of two categories: stuck-open safety relief valves with subsequent re-closure, and primary side pipe breaks.

The NRC previously performed a review to assess the general applicability of the PTS evaluation results from the three individual PWR vendor-designed plants to the population of vendor-designed PWRs [14]. The results from the NRC generalization study were reviewed to confirm

that the transients evaluated in the NRC PTS study for the Westinghouse plant design are applicable to the transients used in this evaluation. The conclusion in the NRC generalization study [14] that the base results for the three individual vendor-designed plants generally are applicable to the population of vendor-specific designs indicates that the transients used by the NRC for the PTS evaluation of the vessel in Westinghouse designed reactors are applicable for the analysis of the Westinghouse designed reactor vessels evaluated in this study.

The PTS and normal cooldown events included in the risk analyses are summarized in Table 3-8. Both the normal cooldown and PTS events were included in the analysis of the RPV beltline, nozzle shell course and heads. Considering the position of the closure head relative to the reactor vessel inlet nozzles and the position of the bottom head relative to the vessel downcomer, application of the PTS transient loads and the normal cooldown loads to the RPV closure and bottom heads is conservative. The PTS transients were not included in the analyses of the S/G and pressurizer components because the PTS transient conditions would not be transmitted directly to these components. Because the scope of this work did not include evaluation of component specific normal operating or transient events for the S/G and pressurizer, the time histories for the reactor vessel shown in Figure 3-8 were used in the evaluation of the S/G channel head and the pressurizer shells and heads. In some instances, detailed PFM analyses for some components were excluded based on the results from deterministic analyses as described in Section 4. The S/G upper and lower shells were not included in the deterministic or PFM analyses but received qualitative evaluations as described in Section 4.

Table 3-8
Loading Conditions Considered in the Risk Evaluation

Forged Component	Normal Cooldown Along Beltline P-T Limit Curve	Pressurized Thermal Shock Transients
Thick wall RPV: beltline shell	Yes	Yes
Thick wall RPV: nozzle shell course	Yes	Yes
Thick wall RPV: head	Yes	Yes
Thin wall RPV: beltline shell	Yes	Yes
Thin wall RPV: nozzle shell course	Yes	Yes
Thin wall RPV: head	Yes	Yes
S/G upper shell	No	No
S/G lower shell	No	No
S/G channel head	Yes	No
Pressurizer shell	Yes	No
Pressurizer head	Yes	No

Neutron Fluence Distribution

The azimuthal fluence distribution at the vessel inner surface was defined using the peak beltline fluences listed in Table 3-1 and a relative fluence map determined from [15]. This relative fluence map is typical of the relative fluence distribution in RPVs at Westinghouse designed plants and previously was used in the NRC PTS study [14, 16].

At any specified azimuthal location, the fluence typically has little variation in the axial direction. Consequently, the fluence at any axial location is set equal to the maximum value at the corresponding azimuthal position. The shape and relative position of the core and vessel wall produce an azimuthal fluence distribution that is symmetrical in 45° segments around the vessel wall. Figure 3-9 shows the relative azimuthal fluence distribution obtained from the fluence map for a 45° segment [15]. The figure includes the histogram representation for the fluence distribution used as input into the FAVOR software for the PFM analysis. The histogram indicates the percentage of vessel circumference that is exposed to each relative fluence level.

The fluence distribution shown in Figure 3-9 was used for the RPV beltline and nozzle shell course regions. For the other components, including the RPV heads, an azimuthal fluence distribution is not applicable and the single fluence value shown in Table 3-1 was used in the analysis.

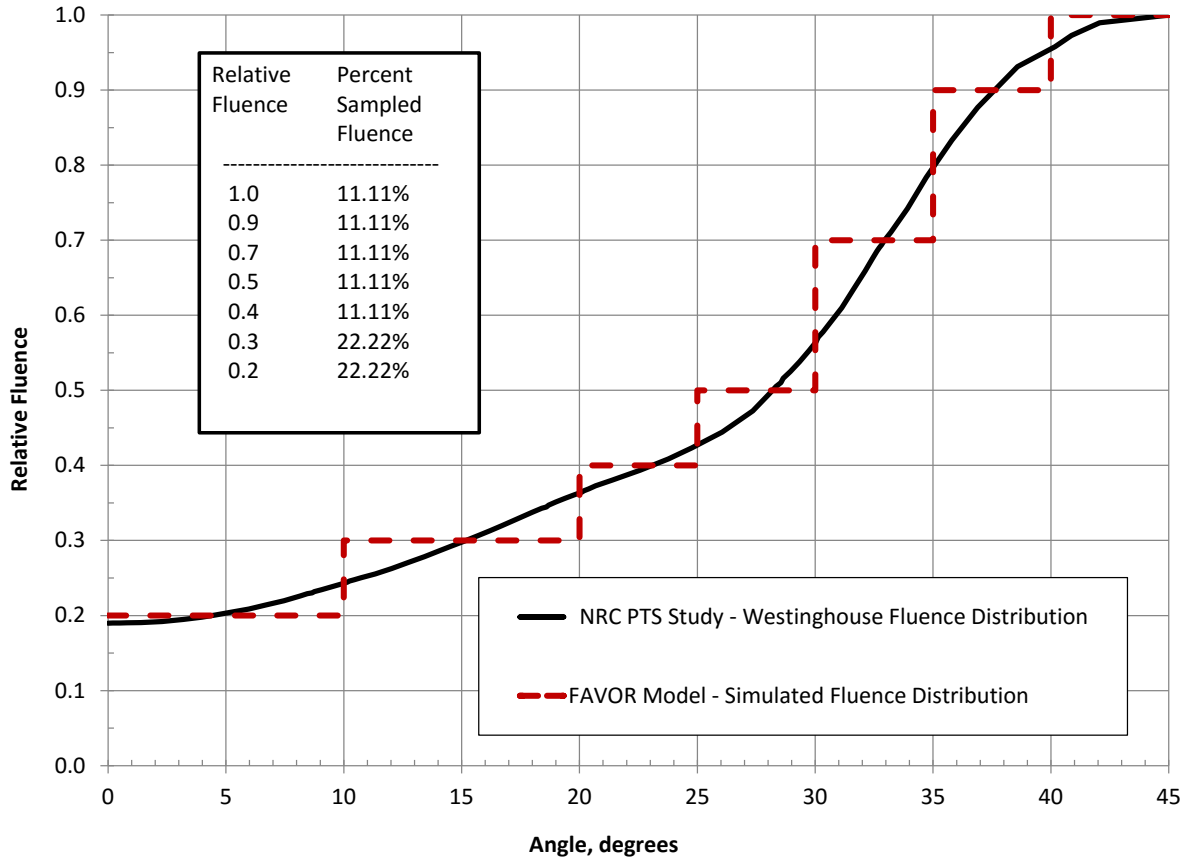

Figure 3-9
Relative RPV Fluence Map and Histogram Used in the FAVOR PFM Calculations

Embedded and Surface Flaw Distributions

The surface and embedded flaw distributions used in the PFM analyses for forgings and welds in the thin and thick wall vessels generally are the same as those used by the NRC during the development of 10CFR50.61a.

Although the same flaw distributions are used in the PFM analyses for the thick and thin wall vessels, the number of sampled flaws in each vessel will be different because the number of flaws in the vessel depends on the volume and inside surface area of the of the vessel wall. There is a total of approximately 4,680 flaws in each thick wall trial vessel and 2,830 flaws in each thin wall trial vessel. Approximately 76% of the flaws in each vessel are embedded flaws in the forging material and 24% of the flaws in each vessel are embedded flaws in the circumferential weld. The weld embedded flaw distribution includes 2% repair welds and has a flaw depth truncation of about 2-inches (51-mm). The forging embedded flaw distribution has a flaw depth truncation of about 0.43-inches (11-mm). Because PTS events produce the most severe combined stress and toughness conditions near the vessel inner surface the PFM analysis uses the embedded flaws located in the inner three-eighths of the vessel wall consistent with conventional practice in the U.S. for evaluating PTS transients [14, 15].

There are approximately two circumferential inner surface flaws sampled in each thick and thin wall trial vessel. The total depth of the postulated inner surface flaws is three percent of the vessel wall thickness, including cladding, which is consistent with the inner surface flaw depth used in the NRC evaluation to define the requirements in 10CFR50.61a. Some component wall thicknesses are relatively small and a flaw depth of three percent of the wall thickness, including cladding, would not be deep enough to penetrate the through the cladding and into the base metal. In these instances, the depth of the surface flaw was set equal to four percent of the wall thickness, including cladding. Generally, inner surface flaws are the dominant contributors to CPF for normal vessel cooldown; consequently, as a computational efficiency, only surface flaws were used in the PFM analysis for the normal vessel cooldown event.

Additional Analysis Input

The irradiation degradation related variables (Cu, Ni, Mn, P, fluence) are sampled by the FAVOR software during the PFM analysis. The standard deviations used for sampling Cu, Ni, Mn, P and fluence are the default values in the FAVOR software [18]. As indicated previously, the standard deviation for $RT_{NDT(U)}$ is determined from Eq. 3-9 for each macrosegregation level ($\Delta C/C_o$) in the macrosegregation distribution.

The FAVOR weld residual stress option was enabled for the analyses in this study. Consistent with the analysis procedure in [15], the FAVOR warm pre-stress option was enabled for the evaluation of the PTS transients. The warm pre-stress option was not enabled for the evaluation of the normal RPV cooldown event to account for the uncertainty in the cooldown path.

The temperature at normal full power operation is 547°F (286°C). The stress free temperature (SFT) used to determine the stress due to stainless steel cladding on the vessel inner surface is 445°F (229°C); the basis for a SFT equal to 445°F (229°C) is presented in Appendix A.

The default values contained in the FAVOR input files for the remaining mechanical and physical properties were used in the PFM analyses.

4
ANALYSIS RESULTS

Deterministic Analyses Results

A series of preliminary deterministic fracture mechanics analyses were performed to help identify the component, load and irradiation conditions that are most likely to have a significant contribution to the CPF and 95% TWCF. Those conditions that were identified as having the potential for contribution to the CPF and 95% TWCF were then evaluated using PFM analyses to obtain the CPF and 95% TWCF as a function of carbon macrosegregation level.

The deterministic analyses were performed for three sets of conditions: ring forgings in high fluence regions, ring forgings in low fluence regions and heads in low fluence regions. The loading used in the deterministic analyses for these three categories is a normal reactor cooldown from 547°F (286°C) to 300°F (149°C) at 100°F/hr. (56°C/hr.), then from 300°F (149°C) to 60°F (16°C) at 50°F/hr. (28°C/hr.), as shown in Figure 3-8. The pressure and temperature time histories used for the S/G channel head and the pressurizer ring and head forgings are the same as the pressure and temperature time histories used in the evaluation of the thin wall (6.7-inches) (170-mm) RPV, as shown in Figure 3-8. The loading for the thin wall vessel was used because it has a higher allowable pressure compared to the thick wall vessel and will result in more conservative loads for the S/G channel head and pressurizer ring and head forgings.

The deterministic analyses used the inner surface flaw depths described in Section 3 with an aspect ratio (ratio of total flaw length to flaw depth) equal to ten.

Ring Forgings in a High Fluence Environment

Figure 4-1 presents the results from the deterministic analyses for the ring forgings in the high fluence environment, including the beltline forgings and circumferential welds in the thick wall (8.45-inch) (215-mm) and thin wall (6.7-inch) (170-mm) reactor pressure vessels.

Figure 4-1 shows the applied stress intensity, K_I, as a function of time during the cooldown, and the material fracture toughness, aK_{Ic}, as a function of time and percent carbon macrosegregation. The applied K_I values shown in the plot are for the region adjacent to the circumferential weld and include the weld residual stress. The fracture toughness, aK_{Ic}, is the lower bound toughness used in the FAVOR software to define the value of applied K_I below which initial extension of the postulated inner surface flaw will not occur [18]. A series of aK_{Ic} curves are plotted as a function of percent carbon macrosegregation to determine where the applied K_I curves intersect the aK_{Ic} curves and at what level of carbon macrosegregation there may be a significant contribution to the CPF.

The results in Figure 4-1 show that the applied K_I curve for the thick vessel beltline is substantially higher than the toughness curve aK_{Ic} at all levels of carbon macrosegregation and, consequently, is likely to have significant contribution to CPF and 95% TWCF. The results in

Figure 4-1 also show that the applied K_I curve for the thin vessel beltline is higher than the toughness curve aK_{Ic} at all levels of carbon macrosegregation, but to a lesser extent compared to the thick wall vessel. Consequently, the thin wall vessel beltline is expected to contribute to the CPF and 95% TWCF, but to a lesser extent than that of the thick wall vessel.

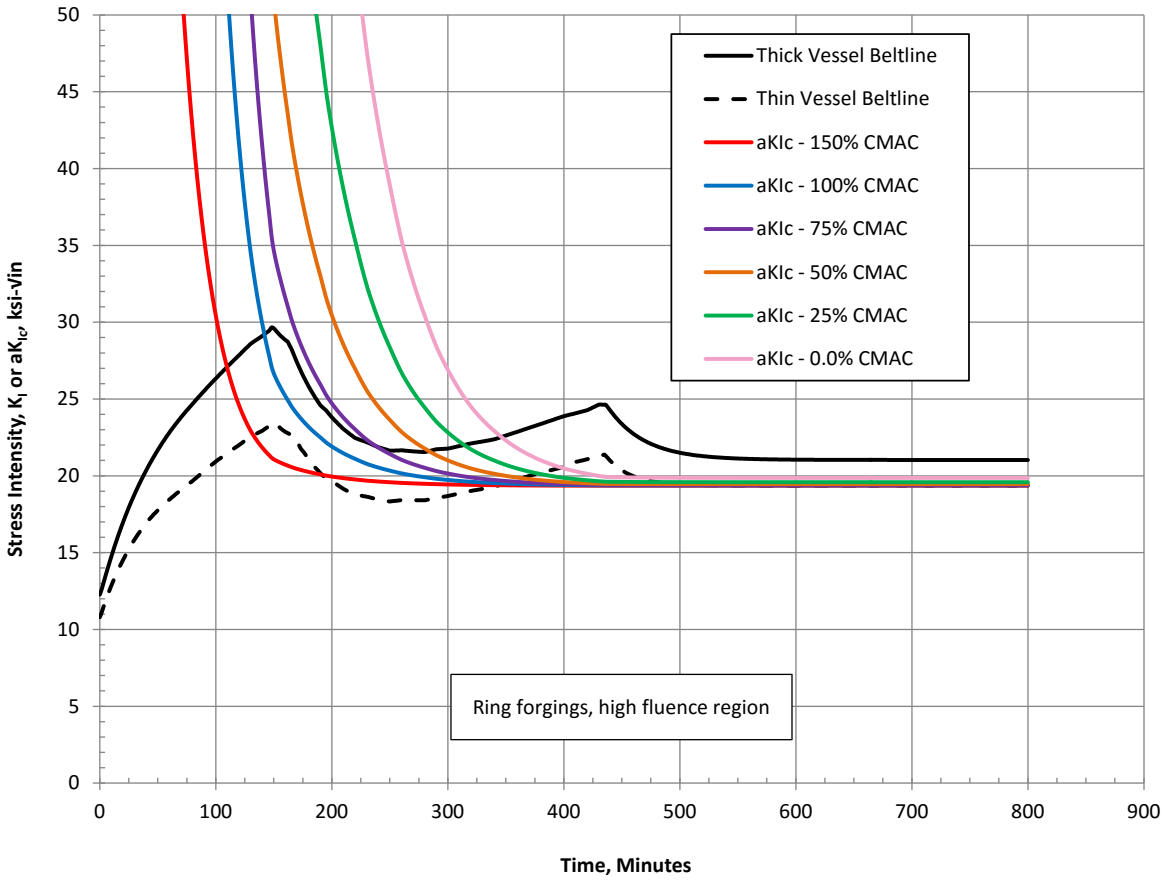

Figure 4-1
Deterministic Results for Ring Forgings in a High Fluence Environment

Ring Forgings in a Low Fluence Environment

Figure 4-2 presents the results from the deterministic analyses for the ring forgings in the low fluence environment, including the pressurizer shell and the RPV nozzle shell course in the thick and thin wall vessels.

Figure 4-2 shows the applied stress intensity, K_I, as a function of time during the cooldown, and the material fracture toughness, aK_{Ic}, as a function of time and percent carbon macrosegregation. The applied K_I values shown in the plot are for the region adjacent to the circumferential weld and include the weld residual stress.

The results in Figure 4-2 show that the applied K_I curve for the thick wall vessel nozzle shell course is higher than the applied K_I curve for the thin wall vessel nozzle shell course, and substantially higher than the applied K_I curve for the pressurizer shell. These results indicate that

both the thick and thin wall vessel nozzle shell courses will contribute to the CPF and 95% TWCF, with the larger contribution coming from the thick wall vessel nozzle shell course.

The applied K_I curve for the pressurizer ring forging likely will never exceed the aK_{Ic} curve during the cooldown, and consequently, the pressurizer ring forging is expected to have no contribution to CPF and 95% TWCF, and was not included in the PFM analyses.

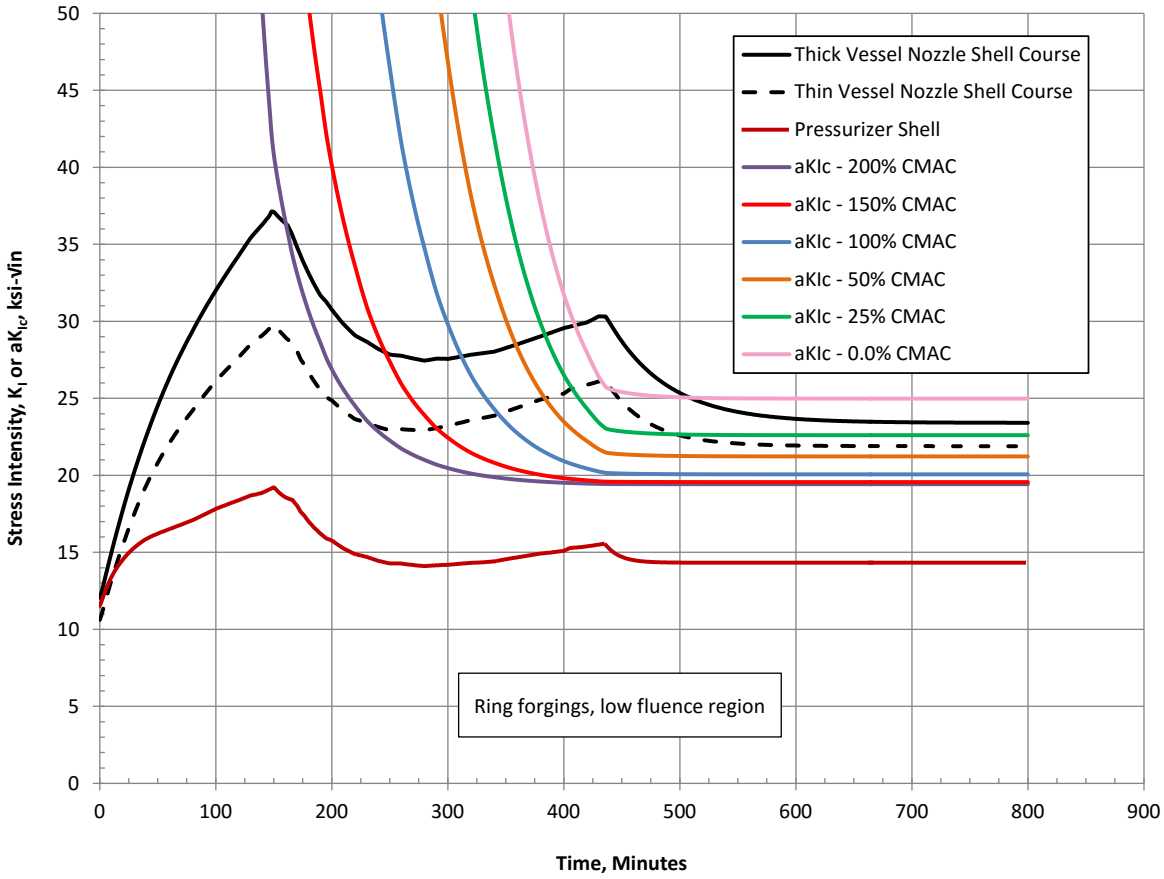

Figure 4-2
Deterministic Results for Ring Forgings in a Low Fluence Environment

Head Forgings in a Low Fluence Environment

Figure 4-3 presents the results from the deterministic analyses for the head forgings in the low fluence environment, including the RPV closure and bottom heads, the S/G channel head and the pressurizer heads. Because there are no welds in the carbon macrosegregation region in the RPV bottom head and the S/G channel head, as illustrated in Figure 3-6, the applied K_I curves shown for the RPV bottom head and S/G head in Figure 4-3 do not include weld residual stress. However, because the pressurizer heads and the RPV closure head contain penetrations and welds in the macrosegregation region, the applied K_I for the pressurizer heads and the RPV closure head include the weld residual stress.

As shown in Figure 4-3, the closure head for the thick wall vessel and the S/G channel head have applied K_I curves that exceed the aK_{Ic} curve and have the potential to contribute to the CPF and

95% TWCF. The applied K_I curves for the thin wall vessel closure head and pressurizer heads never exceed the aK_{Ic} curve during the cooldown, and consequently, the thin wall vessel closure head and the pressurizer heads are not expected to contribute to the CPF and 95% TWCF. Although not shown in Figure 4-3, the applied K_I curves for the thick and thin wall vessel bottom heads lay below the applied K_I curve for the thin wall vessel closure head. Consequently, the RPV bottom heads are not expected to make a significant contribution to the CPF and 95% TWCF. The S/G channel head has a relatively high applied K_I because the S/G channel head wall thickness is greater than the thickness of the other heads and has higher thermal stress and K_I for the same normal cooldown rate. The thick wall vessel closure head has a high applied K_I because the closure head is relatively thick (7-inches) (178-mm) and has a relatively high thermal stress, and includes the weld residual stress.

Based on the results in Figure 4-3, PFM analyses were not performed for the pressurizer heads.

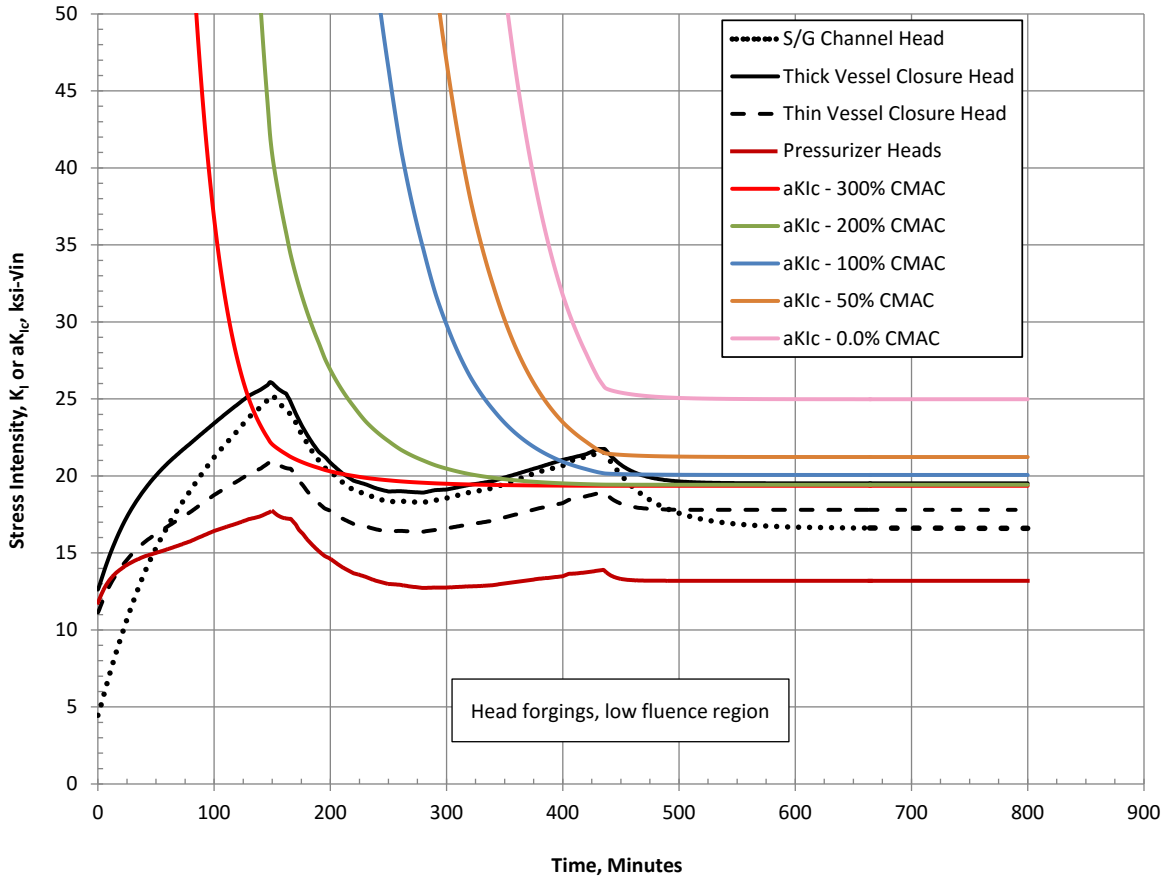

Figure 4-3
Deterministic Results for Head Forgings in a Low Fluence Environment

PFM Analysis Results

Based on the results from the deterministic analyses, PFM analyses were performed for the RPV beltline and nozzle shell course ring forgings, and the RPV and S/G head forgings using the procedures and analysis input described in Section 3.

During the PFM analyses it was determined that the risk contributions for ring and head forgings were less than the risk criteria CPF = 1E-6 and 95% TWCF = 1E-6 yr^{-1} for the measured macrosegregation distributions shown in Figure 3-5 for ring forgings and Figure 3-6 for head forgings. To determine the carbon macrosegregation distributions that would provide CPF = 1E-6 and 95% TWCF = 1E-6 yr^{-1} for head and ring forgings, the macrosegregation values in the $\Delta C/C_o$ bins in Figure 3-5 and Figure 3-6 were multiplied by a factor to obtain higher values of CPF and 95% TWCF. The same multiplier was used to increase $\Delta C/C_o$ for each shell segment except for Segment A, which is assumed to always be free of carbon macrosegregation. This process was repeated several times to provide a curve of CPF or 95% TWCF as a function of the maximum percent carbon macrosegregation in each of the scaled distributions. Even though the CPF and 95% TWCF are plotted as a function of the distribution maximum values of $\Delta C/C_o$, the CPF and TWCF calculations include all the $\Delta C/C_o$ values in the distribution.

In a number of instances, factors greater than 3 on the measured macrosegregation distributions shown in Figure 3-5 for ring forgings and Figure 3-6 for head forgings were needed to meet the risk criteria CPF = 1E-6 or 95% TWCF = 1E-6 yr^{-1}. Based on previous extensive work [4,5,7,8,10,12], percent carbon macrosegregation levels more than 3 times the measured values are not considered credible, and calculated values of CPF or 95% TWCF were not considered in the risk evaluation at postulated macrosegregation levels greater than 3 times the measured values shown in Figure 3-5 and Figure 3-6.

Thick Wall Reactor Pressure Vessel

Normal RPV Cooldown

Figure 4-4 presents the results from the PFM analysis for the RPV components in the thick wall (8.45-inches) (215-mm) vessel during a normal cooldown along the Appendix G allowable P-T limit curve, where the CPF is plotted as a function of the distribution maximum value of percent carbon macrosegregation.

The results in Figure 4-4 indicate that the beltline and nozzle shell course regions provide similar contributions to risk in the range from 25% to 75% carbon macrosegregation. Similar levels of risk are provided by the closure head in the range from 250% to 300% carbon macrosegregation. The risk provided by the RPV bottom head is negligible compared to the risk contribution from the closure head.

The risk of interest for RPV integrity is the sum of the risk contributions from the major RPV components shown in Figure 4-4. Because there are a large number of possible combinations that can be used to calculate the total RPV risk, a few examples are provided to illustrate the margins on CPF relative to the risk criterion CPF = 1E-6, and the margins on the carbon macrosegregation level relative to the measured macrosegregation distributions shown for ring forgings in Figure 3-5 and for head forgings in Figure 3-6.

First, if all the ring forgings in the thick wall vessel have the distribution maximum measured value of 25% carbon macrosegregation and all the head forgings in the thick wall vessel have the distribution maximum measured value of 100% carbon macrosegregation, then the total CPF for the vessel is approximately 1E-7.

Second, if all the ring forgings in the thick wall vessel have twice the distribution maximum measured value of carbon macrosegregation (50%) and all the head forgings in the thick wall vessel have twice the distribution maximum measured value of carbon macrosegregation (200%), then the total CPF for the vessel is approximately 4.6E-7.

Finally, if all the ring forgings in the thick wall vessel have 2.6 times the distribution maximum measured value of carbon macrosegregation (65%) and all the head forgings in the thick wall vessel have 2.6 times the distribution maximum measured value of carbon macrosegregation (260%), then the total CPF for the vessel is approximately 1E-6.

These examples show that there is an order of magnitude margin on CPF relative to the risk criterion CPF = 1E-6 when all the RPV forgings have the measured macrosegregation distributions shown in Figure 3-5 and Figure 3-6. Similarly, the examples show that there is a margin of 2.6 on the measured carbon macrosegregation distributions in Figure 3-5 and Figure 3-6 when CPF = 1E-6.

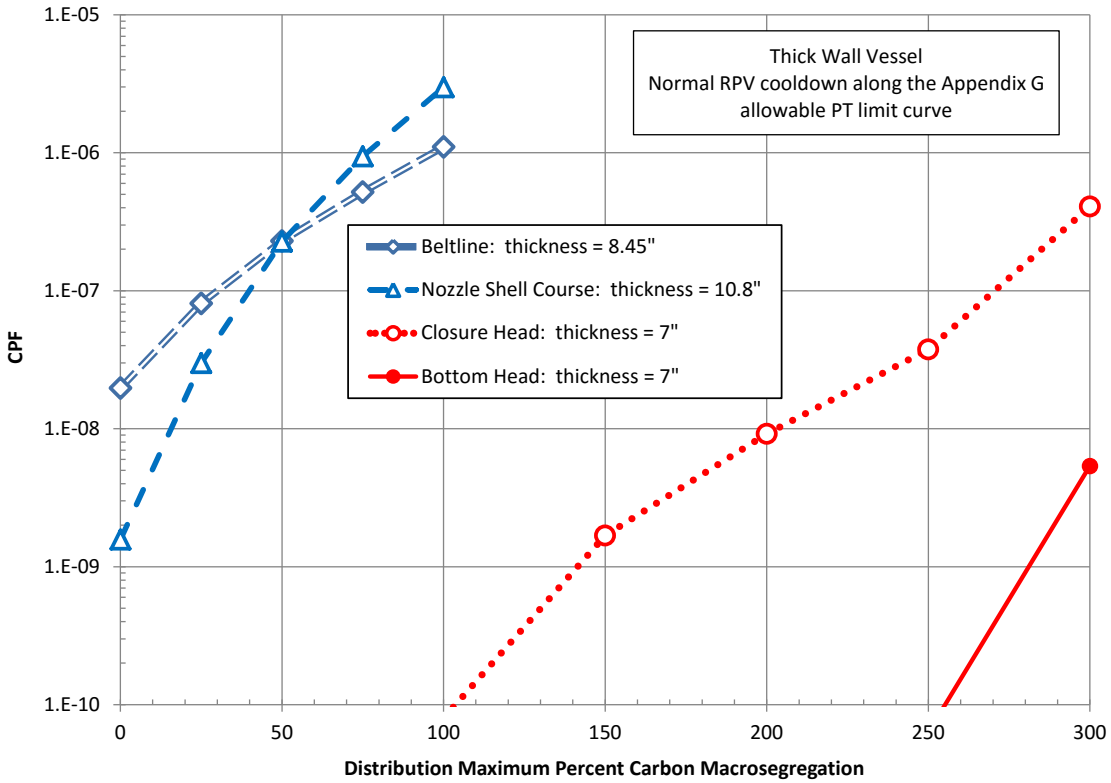

Figure 4-4
PFM Results for the Thick Wall Pressure Vessel, Normal RPV Cooldown

Postulated PTS Events

Figure 4-5 presents the results from the PFM analysis for the RPV components in the thick wall (8.45-inches) (215-mm) vessel for the postulated PTS transient events, where the 95% TWCF is plotted as a function of the distribution maximum value of percent carbon macrosegregation.

The results in Figure 4-5 indicate that the beltline ring forgings have a 95% TWCF ranging from about 3E-9 yr^{-1} at 25% carbon macrosegregation to about 1E-6 yr^{-1}at 75% macrosegregation. Similar levels of risk are provided by the closure head in the range from 200% to 260% carbon macrosegregation, and by the bottom head in the range from 240% to 300% carbon macrosegregation. The 95% TWCF for the RPV nozzle shell course is less than 1E-10 yr^{-1} at carbon macrosegregation levels beyond 3 times the measured distribution values for ring forgings and is negligible.

The data in Figure 4-5 show that if all the ring forgings in the thick wall vessel have the distribution maximum measured value of 25% carbon macrosegregation and all the head forgings in the thick wall vessel have the distribution maximum measured value of 100% carbon macrosegregation, then the total 95% TWCF for the vessel is dominated by the risk contribution from the beltline forgings and is approximately 3E-9 yr^{-1}.

The results in Figure 4-5 also indicate that if all the ring forgings in the thick wall vessel have twice the distribution maximum measured value of carbon macrosegregation (50%) and all the head forgings in the thick wall vessel have twice the distribution maximum measured value of carbon macrosegregation (200%), then the total 95% TWCF for the vessel is again dominated by the risk contribution from the beltline forgings and is approximately 9E-8 yr^{-1}.

The information in Figure 4-5 also shows that if all the ring forgings in the thick wall vessel have 2.5 times the distribution maximum measured value of carbon macrosegregation (62.5%) and all the head forgings in the thick wall vessel have 2.5 times the distribution maximum measured value of carbon macrosegregation (250%), then the total 95% TWCF for the vessel is approximately 1E-6 yr^{-1}.

These results show that there are more than two orders of magnitude margin on 95% TWCF relative to the risk criterion 95% TWCF = 1E-6 yr^{-1} when the RPV forgings have the measured macrosegregation distributions shown in Figure 3-5 and Figure 3-6. Similarly, the results indicate that there is a margin of 2.5 on the measured carbon macrosegregation distributions in Figure 3-5 and Figure 3-6 when 95% TWCF = 1E-6 yr^{-1}.

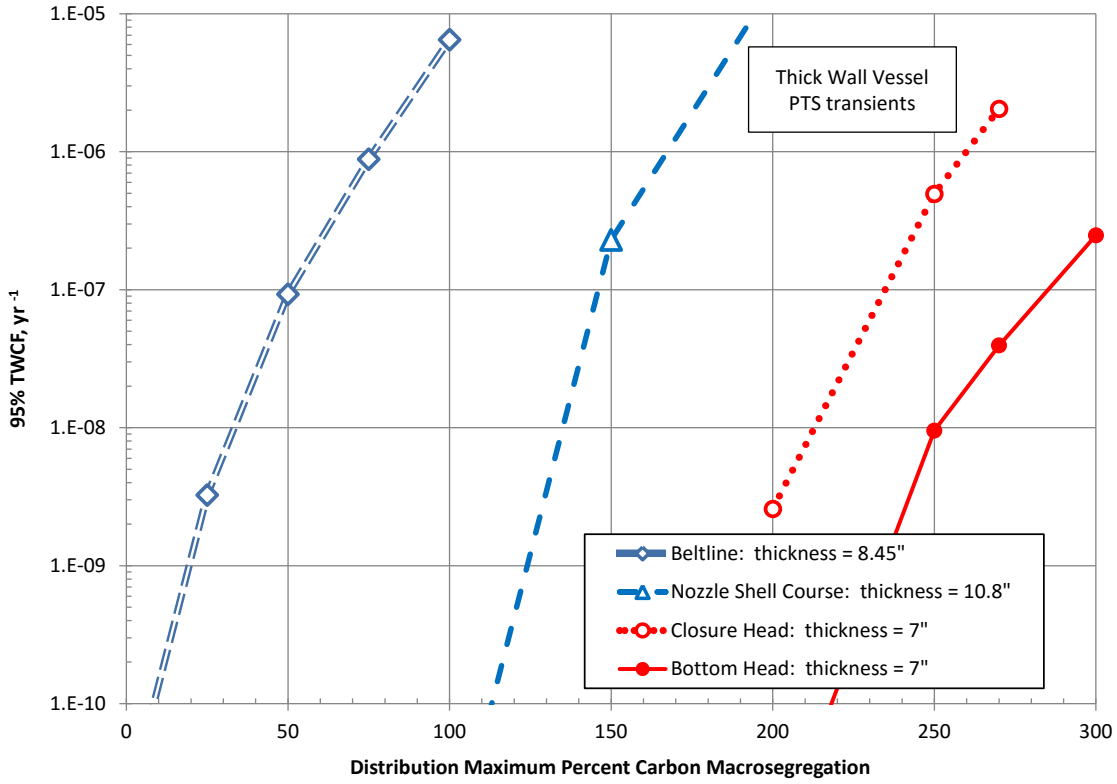

Figure 4-5
PFM Results for the Thick Wall Pressure Vessel, PTS Transients

Thin Wall Reactor Pressure Vessel

Normal RPV Cooldown

Figure 4-6 presents the results from the PFM analysis for the RPV components in the thin wall (6.7-inches) (170-mm) vessel during a normal cooldown along the Appendix G allowable P-T limit curve, where the CPF is plotted as a function of the distribution maximum value of percent carbon macrosegregation.

The results in Figure 4-6 indicate that the CPF for the nozzle shell course forging ranges from about 3E-10 at 25% macrosegregation to about 3E-8 at 75% macrosegregation, while the CPF for the beltline forgings ranges from about 3E-10 at 25% macrosegregation to about 2E-9 at 75% macrosegregation. The results in Figure 4-6 also indicate that the contribution to risk from the closure head is negligible. The risk contribution from the bottom head is also negligible, and does not appear in Figure 4-6 because the CPF is less than 1E-10 at 300% carbon macrosegregation.

The results in Figure 4-6 show that if all the ring forgings in the thin wall vessel have the distribution maximum measured value of 25% carbon macrosegregation and all the head

forgings in the thin wall vessel have the distribution maximum measured value of 100% carbon macrosegregation, then the total CPF is approximately 7E-10.

Similarly, if all the ring forgings in the thin wall vessel have twice the distribution maximum measured value of carbon macrosegregation (50%) and all the head forgings in the thin wall vessel have twice the distribution maximum measured value of carbon macrosegregation (200%), then the total CPF for the vessel is approximately 6E-9.

Finally, the carbon macrosegregation distribution levels necessary to reach the risk criterion, CPF = 1E-6 for RPV cooldown are greater than 3 times the measured carbon macrosegregation distribution levels shown in Figure 3-5 and Figure 3-6.

These results show that there are approximately three orders of magnitude margin on CPF relative to the risk criterion CPF = 1E-6 when all the RPV forgings have the measured macrosegregation distributions shown in Figure 3-5 and Figure 3-6. Similarly, there is a margin of more than 3 on the measured carbon macrosegregation distributions in Figure 3-5 and Figure 3-6 when CPF = 1E-6.

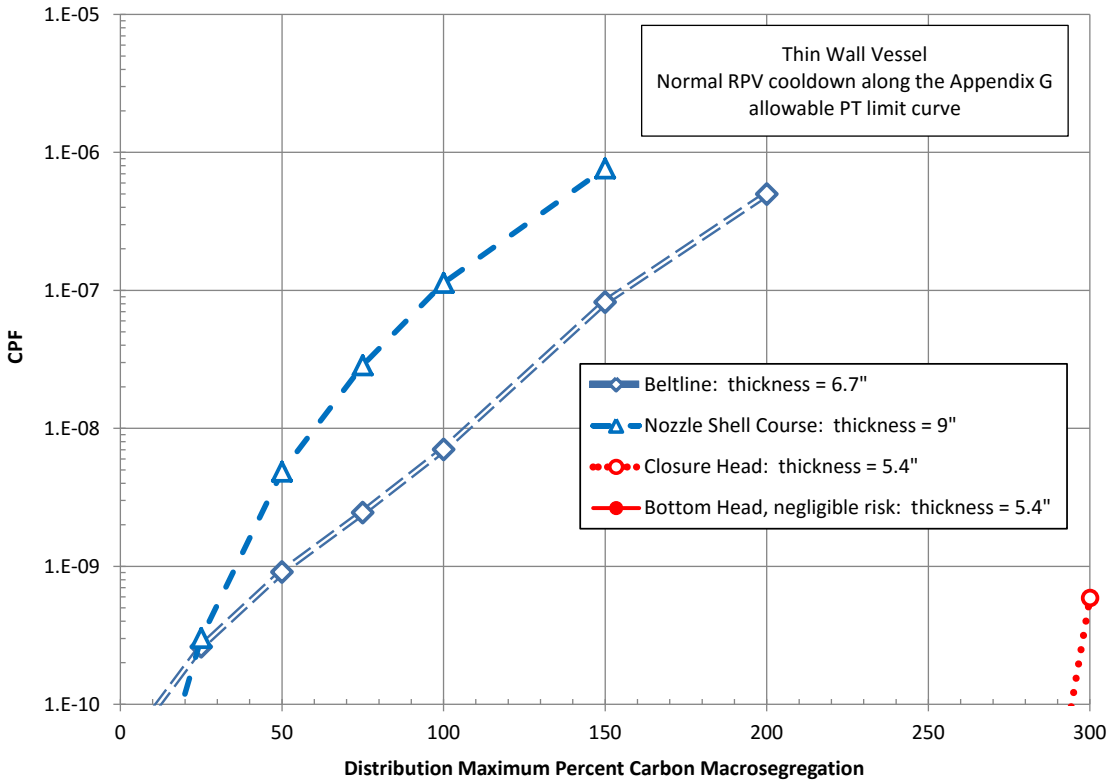

Figure 4-6
PFM Results for the Thin Wall Pressure Vessel, Normal RPV Cooldown

Postulated PTS Transients

Figure 4-7 presents the results from the PFM analysis for the RPV components in the thin wall (6.7-inches) (170-mm) vessel for the PTS transient events, where the 95% TWCF is plotted as a function of the distribution maximum value of percent carbon macrosegregation.

The results in Figure 4-7 indicate that the beltline ring forgings have 95% TWCF ranging from less than 1E-10 yr^{-1} at macrosegregation levels less than about 60% to about 4E-9 yr^{-1} at 75% macrosegregation, and are the dominant contributors to risk compared to the nozzle shell course ring forging. Similar levels of risk are provided by the closure head in the range from about 240% to 300% carbon macrosegregation. Results for the bottom head are not shown in Figure 4-7 because the 95% TWCF is less than 1E-10 yr^{-1} at 300% carbon macrosegregation.

The results in Figure 4-7 also show that if the ring forgings in the thin wall vessel have twice the distribution maximum measured value of carbon macrosegregation (50%) and all the head forgings in the thick wall vessel have twice the distribution maximum measured value of carbon macrosegregation (200%), then the total CPF for the vessel is less than 1E-10 yr^{-1}.

Finally, the results show that the carbon macrosegregation distribution levels necessary to reach the risk criterion, 95% TWCF = 1E-6 yr^{-1} for the postulated PTS events are greater than 3 times the measured carbon macrosegregation distribution levels shown in Figure 3-5 and Figure 3-6.

These results show that there are more than four orders of magnitude margin on CPF relative to the risk criterion CPF = 1E-6 when all the RPV forgings have the measured macrosegregation distributions shown in Figure 3-5 and Figure 3-6. Similarly, the results indicate that there is a margin of more than 3 on the measured carbon macrosegregation distributions in Figure 3-5 and Figure 3-6 when 95% TWCF = 1E-6 yr^{-1}.

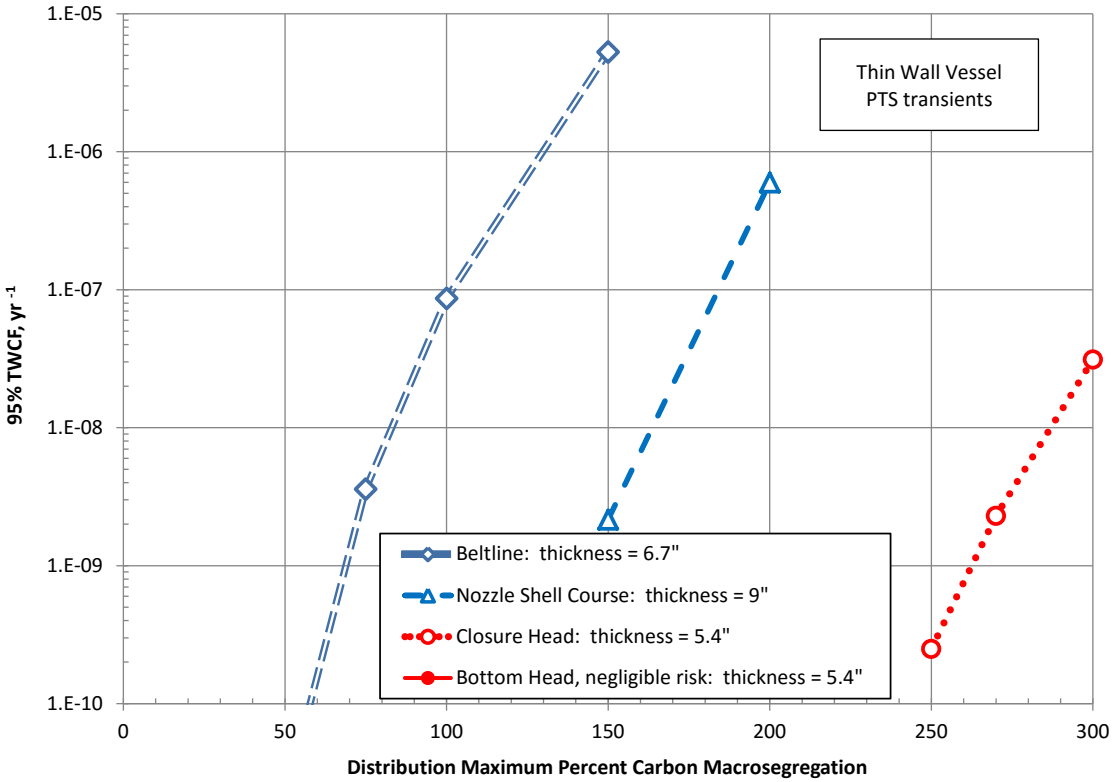

Figure 4-7
PFM Results for the Thin Wall Pressure Vessel, PTS Transients

S/G Channel Head

Normal RPV Cooldown

Figure 4-8 presents the results from the PFM analysis for the S/G channel head, where the CPF is plotted as a function of the distribution maximum value of carbon macrosegregation in the distribution illustrated in Figure 3-6 for head forgings. The PFM analysis of the channel head was performed for a cooldown event with the pressure and temperature time histories shown in Figure 3-8 for the thin wall (6.7-inches) (170-mm) RPV.

The results in Figure 4-8 show that if the S/G channel head forging has the distribution maximum measured value of 100% carbon macrosegregation, then the total CPF is approximately 3E-9.

Similarly, if the S/G channel head forging has twice the distribution maximum measured value (200%), then the total CPF for the vessel is approximately 1E-7.

The information in Figure 4-8 also shows that if the S/G head forging has 3 times the distribution maximum measured value of carbon macrosegregation (300%), then the total CPF for the vessel is approximately 1E-6.

These results show that there are more than two orders of magnitude margin on CPF relative to the risk criterion CPF = 1E-6 when the S/G channel head forging has the measured carbon macrosegregation distribution shown in Figure 3-6. Similarly, there is a margin of approximately 3 on the measured carbon macrosegregation distribution shown in Figure 3-6 for the S/G channel head when CPF = 1E-6.

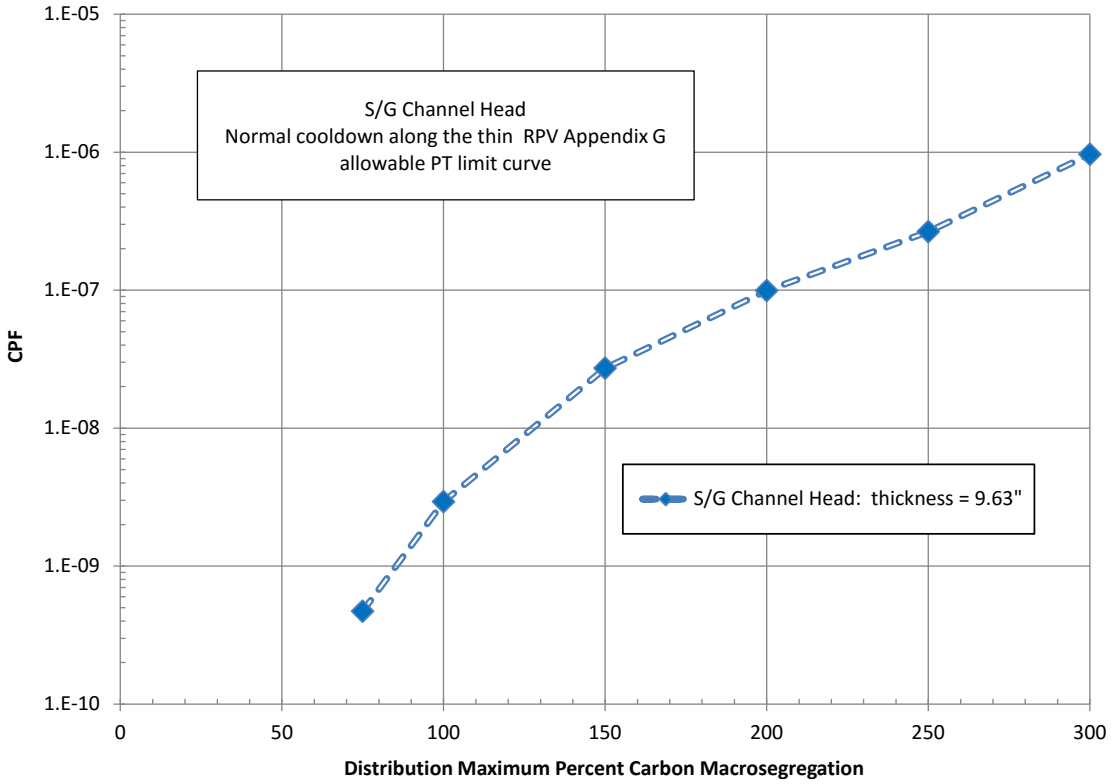

Figure 4-8
PFM Results for the S/G Channel Head, Thin Wall RPV Normal Cooldown Pressure–Temperature Time Histories

Conservatisms in the PFM Analyses

The PFM results shown in Figure 4-4 through Figure 4-8 have been obtained using a number of conservative assumptions, including: at any given height, the macrosegregation distribution extends uniformly through the entire vessel wall thickness; all the ring forgings have the same carbon macrosegregation distribution simultaneously; all the head forgings have the same carbon macrosegregation distribution simultaneously; all components have the limiting material; and, except for the RPV bottom head and the S/G channel head, the forging segments attached to the weld have the highest level of macrosegregation in the macrosegregation distribution. These conservative assumptions provide added assurance that there are substantial margins against failure through an 80-year operating period when conservative distributions of carbon

macrosegregation are postulated to be present in the RPV, S/G and pressurizer head and ring forgings in PWRs.

Qualitative Analysis Results

S/G Upper and Lower Shell Ring Forgings

As indicated in Section 2, carbon macrosegregation was detected in several S/G shell ring forgings in France. Based on the results from the deterministic and PFM analyses presented earlier in this section, a qualitative assessment was made of the risk of S/G shell ring forgings with postulated carbon macrosegregation.

First, the S/G upper shell has an inner radius = 80-inches (2032-mm) and thickness = 3.5-inches (89-mm), and the lower S/G shell has an inner radius = 60-inches (1524-mm) and thickness = 2.6-inches (66-mm). In both instances the ratio of radius to thickness (R/t) is approximately 23, which is roughly twice that of the RPV. Since the pressure in the S/G shells is about half the pressure in the RPV, then the pressure stress in the S/G shell and the RPV beltline shell are about the same. The residual stress at the circumferential weld in the S/G shell also should be approximately equal to the residual weld stress in the RPV beltline. In addition, the inner surfaces of the S/G upper and lower shells are not exposed to primary water and are not clad; consequently, stresses due to cladding are absent in the S/G shell. Because the S/G shell ring forging thicknesses are less than the thin wall RPV and pressurizer shell thicknesses, then the thermal stresses in the S/G shell are lower than the thermal stresses in the thin wall RPV and pressurizer shells. Overall then, the stresses in the S/G shells are significantly lower than those in the thin wall RPV and the pressurizer shells. Second, there is no significant radiation exposure to the S/G shell so the RT_{MAX} will be much lower than that of the RPV beltline. The combination of the lower stress and lower RT_{MAX} relative to the thin wall RPV indicates that the CPF is substantially less than = 1E-6 for S/G shell ring forgings with postulated carbon macrosegregation up to at least 3 times the measured values.

Analysis Results – Summary Overview

This section summarizes the results from the qualitative risk evaluations and the quantitative deterministic and PFM risk evaluations for the components with head or ring forgings.

Table 4-1 provides a qualitative overview of the component and load conditions that contribute to risk from postulated carbon macrosegregation in the RPV, S/G and pressurizer. The criteria used to define the component and load conditions identified as risk contributors include components and loads where either the CPF is approximately ≥ 1E-7 or the 95% TWCF is approximately ≥ 1E-7 yr^{-1}, at macrosegregation levels less than 3 times the measured macrosegregation distributions shown in Figure 3-5 for ring forgings and in Figure 3-6 for head forgings. These criteria provide a conservative and inclusive definition of the components and load conditions that contribute to risk for postulated macrosegregation.

Table 4-1
Forged Components that Contribute to Risk from the Presence of Postulated Carbon Macrosegregation

Forged Component	Contribution to Risk at Three Times the Measured Carbon Macrosegregation Distribution	
	Cooldown Loads	PTS Transients
Thick wall RPV: beltline ring forging	Yes	Yes
Thick wall RPV: nozzle shell course ring forging	Yes	No
Thick wall RPV: closure head forging	Yes	Yes
Thick wall RPV: bottom head forging	No	Yes
Thin wall RPV: beltline ring forging	No	No
Thin wall RPV: nozzle shell course ring forging	No	No
Thin wall RPV: closure head forging	No	No
Thin wall RPV: bottom head forging	No	No
S/G: upper shell ring forging	No	n/a
S/G: lower shell ring forging	No	n/a
S/G: channel head forging	Yes	n/a
Pressurizer: shell ring forging	No	n/a
Pressurizer: head forging	No	n/a

5
SUMMARY AND CONCLUSIONS

Carbon macrosegregation is a phenomenon that produces elevated carbon content in extended regions of large steel ingots as the molten metal cools and solidifies in the mold. Various inspections and analytical and experimental studies in France show that positive carbon macrosegregation can occur in various large nuclear components, including RPV heads and S/G ring forgings and channel heads. Macrosegregation in large steel ingots can increase the material carbon, copper and phosphorus contents and reduce the material fracture toughness over extended portions of large, forged structural components in nuclear reactor systems.

Although macrosegregation has not been identified in large forged components at operating reactors in the United States, the Materials Reliability Program (MRP) has performed PFM and risk evaluations to demonstrate that acceptable levels of risk are maintained through the end of an 80-year operating interval for large forged components having postulated macrosegregation in PWRs. The forged components evaluated in the MRP work include the RPV head forgings and beltline and nozzle shell course ring forgings, and S/G and pressurizer head and ring forgings.

The risk evaluations included conservative load and flaw conditions that previously have been used by industry and regulatory authorities in the U.S. for RPV risk evaluations, and conservative carbon macrosegregation distributions obtained from measured data published by French researchers and regulatory authorities for both ring and head forgings. Consistent with the risk goals previously used to define Alternate PTS Rule, 10CFR50.61a [9], and other previous work for assessing RPV integrity [13], the MRP risk evaluations were performed to determine the maximum carbon content that will ensure the 95% TWCF $\leq$ 1E-6 yr^{-1} or that the CPF < 1E-6 for large forgings with postulated carbon macrosegregation. The following conclusions were obtained from this work.

1. The thick wall (8.45-inches) (318-mm) vessel has CPF = 1E-7 for the RPV cooldown when the RPV ring forgings have the measured macrosegregation distribution shown in Figure 3-5 and head forgings have the measured macrosegregation distribution shown Figure 3-6. The carbon macrosegregation distribution levels necessary to reach the risk criterion, CPF = 1E-6, for RPV cooldown are approximately 2.6 times the measured carbon macrosegregation distribution levels.
2. The thick wall vessel has 95% TWCF = 3E-9 yr^{-1} for the postulated PTS transients when the RPV ring forgings have the measured macrosegregation distribution shown in Figure 3-5 and head forgings have the measured macrosegregation distribution shown Figure 3-6. The carbon macrosegregation distribution levels necessary to reach the risk criterion, 95% TWCF = 1E-6 yr^{-1}, for the postulated PTS events are approximately 2.5 times the measured carbon macrosegregation distribution levels.
3. The thin wall (6.7-inches) (170-mm) vessel has CPF = 7E-10 for the RPV cooldown when the RPV ring forgings have the measured macrosegregation distribution shown in Figure 3-5 and head forgings have the measured macrosegregation distribution shown Figure 3-6. The

carbon macrosegregation distribution levels necessary to reach the risk criterion, CPF = 1E-6, for RPV cooldown are greater than 3 times the measured carbon macrosegregation distribution levels.

4. The thin wall vessel has 95% TWCF < 1E-10 yr^{-1} for the postulated PTS transients when the RPV ring forgings have the measured macrosegregation distribution shown in Figure 3-5 and head forgings have the measured macrosegregation distribution shown Figure 3-6. The carbon macrosegregation distribution levels necessary to reach the risk criterion, 95% TWCF = 1E-6 yr^{-1}, for the postulated PTS events are greater than 3 times the measured carbon macrosegregation distribution levels.
5. The S/G channel head (9.63-inch wall) (245-mm) has CPF = 3E-9 for cooldown along the Appendix G allowable P-T limit curve for the thin wall vessel when the head forging has the measured macrosegregation distributions shown in Figure 3-6. The carbon macrosegregation distribution levels necessary to reach the risk criterion, CPF = 1E-6, for normal cooldown is approximately 3 times the measured carbon macrosegregation distribution levels.
6. There are negligible contributions to risk from postulated carbon macrosegregation in the pressurizer head and ring forgings, and S/G ring forgings.
7. The results from this work indicate that there is substantial margin against failure through an 80-year operating interval when conservative distributions of carbon macrosegregation are postulated to be present in the RPV, S/G and pressurizer head and ring forgings in PWRs.
8. The PFM results presented in this work have been obtained using a number of conservative assumptions, including: the macrosegregation distribution extends uniformly through the entire vessel wall thickness; all the ring forgings have the same carbon macrosegregation distribution simultaneously; all the head forgings have the same carbon macrosegregation distribution simultaneously; all components have the limiting material; and, except for the RPV bottom head and the S/G channel head, the forging segments attached to the weld have the highest level of macrosegregation in the macrosegregation distribution. These conservative assumptions provide added assurance that there are substantial margins against failure through an 80-year operating period when conservative distributions of carbon macrosegregation are postulated to be present in the RPV, S/G and pressurizer head and ring forgings in PWRs.

6
REFERENCES

1. E. J. Pickering, "Macrosegregation in Steel Ingots: The Applicability of Modelling and Characterization Techniques," ISIJ International, Vol. 53 (2013), No. 6, pp. 935–949.
2. B. Bramfitt, Structure/Property Relationships in Irons and Steels, Metals Handbook Desk Edition, 2nd Edition, ASM International, 1998.
3. Liu, H. and Zhang, H. (2015) The Influence of Carbon Content and Cooling Rate on The Toughness of Mn-Mo-Ni Low-Alloy Steels, in HSLA Steels 2015, Microalloying 2015 & Offshore Engineering Steels 2015: Conference Proceedings (ed TMS), John Wiley & Sons, Inc., Hoboken, NJ, USA. doi: 10.1002/9781119223399.ch25.
4. "Report to the Advisory Committee of Experts for Nuclear Pressure Equipment: Analysis of the procedure proposed by AREVA to prove adequate toughness of the domes of the Flamanville 3 EPR reactor pressure vessel (RPV) lower head and closure head," ASN/IRSN report CODEP-DEP-2015-037971 ─ IRSN Report /2015-00010, Public Version, l'Autorité de sûreté nucléaire (ASN), France, September 16, 2015.
5. "Summary report for the Advisory Committee of experts for nuclear pressure equipment: Procedure proposed by Areva to prove adequate toughness of the domes of the Flamanville 3 EPR reactor pressure vessel bottom head and closure head – Interim review," ASN/IRSN report CODEP-DEP-2016-019209 ─ IRSN Report /2016-00005, English translation, l'Autorité de sûreté nucléaire (ASN), France, June 17, 2016.
6. Bethmont, M, Frund, JM, Housin, J, and Soular, P, The Toughness of Irradiated Pressure Water Reactor (PWR) Vessel Shell Rings and the Effect of Segregation Zones, ASTM STP 1270, American Society for Testing and Materials, 1996.
7. Press Release, "Additional inspections required on steam generators of five EDF reactors," l'Autorité de sûreté nucléaire (ASN), October 19, 2016, http:// www.french-nuclear-safety.fr/layout/set/print/content/view/full/144722.
8. l'Autorité de sûreté nucléaire (ASN), "Anomalies and Irregularities in Nuclear Pressure Equipment," presentation to the Parliamentary Office for the Assessment of Science and Technology Options (OPECST), France, October 25, 2016.
9. Alternate Fracture Toughness Requirements for Protection Against Pressurized Thermal Shock Events, 10 CFR 50.61a, U.S. Nuclear Regulatory Commission, Federal Register/Vol. 75, No. 1/Monday, January 4, 2010/Rules and Regulations, pp. 13-29.
10. l'Autorité de sûreté nucléaire (ASN), "Recent Developments in Creusot Forge Manufacturing Issues," presentation at the 4th Bilateral Meeting NRA-ASN, Tokyo, Japan, September 12-13, 2016.
11. Nuclear Regulation Authority, "Actions Taken in Japan," presentation at the 4th Bilateral Meeting ASN-NRA, Tokyo, Japan, September 12, 2016.

12. S. Saillet, N. Rupa and C. Benhamou, Impact Of Large Forging Macrosegregations On The Reactor Pressure Vessel Surveillance Program, Fontevraud 6, September 2006.
13. *Assessment of the Use of NUREG-0800 Branch Technical Position 5-3 Estimation Methods for Initial Fracture Toughness Properties of Reactor Pressure Vessel Steels (MRP-401 and BWRVIP-287).* EPRI, Palo Alto, CA: 2015. 3002005348.
14. Technical Basis for the Revision of the Pressurized Thermal Shock (PTS) Screening Limit in the PTS Rule (10 CFR 50.61) NUREG-1806, Vol. 1, August 2007.
15. Technical Basis for Revision of the Pressurized Thermal Shock (PTS) Screening Limit in the PTS Rule (10 CFR 50.61), NUREG-1806, Vol. 2- Appendix A, U.S. Nuclear Regulatory Commission, August 2007.
16. Recommended Screening Limits for Pressurized Thermal Shock (PTS), NUREG-1874, U.S. Nuclear Regulatory Commission, March 2010.
17. ASME Boiler and Pressure Vessel Code, Section XI, Appendix G, "Fracture Toughness Criteria for Protection Against Failure, American Society of Mechanical Engineers.
18. P.T. Williams, T.L. Dickson, B.R. Bass, and H.B. Klasky, Fracture Analysis of Vessels – Oak Ridge FAVOR, v16.1, Computer Code: Theory and Implementation of Algorithms, Methods, and Correlations, ORNL/TM-2016/309, Oak Ridge National Laboratory, Oak Ridge, TN, September, 2016.
19. *Evaluation of the Reactor Vessel Beltline Shell Forgings of Operating U.S. RPVs for Quasi-Laminar Indications (MRP-367).* EPRI, Palo Alto, CA: 2013. 3002000647.
20. "Rules for Construction of Nuclear Facility Components," ASME Boiler and Pressure Vessel Code, Section III, Subparagraph NB-2331, American Society of Mechanical Engineers (ASME).
21. U.S. Nuclear Regulatory Commission, Standard Review Plan, NUREG-0800, Branch Technical Position 5-3, Rev. 2, March 2007.
22. Regulatory Guide 1.99, Revision 2, "Radiation Embrittlement of Reactor Vessel Materials," U.S. Nuclear Regulatory Commission, May 1988.

A
STRESS FREE TEMPERATURE

A thin layer of stainless steel cladding is deposited on the inner surfaces of ferritic steels in some pressure retaining components in reactor systems to prevent corrosion of the surfaces that are exposed to reactor coolant. Because there is a difference between the thermal expansion coefficients for the ferritic and stainless steels, there can be a significant residual stress gradient at the interface between the stainless steel cladding and the ferritic steel, commonly referred to as the cladding to base metal interface (CBMI). The residual stress due to the presence of the cladding can produce high values of applied stress intensity, K_I, for small surface flaws whose depth extends through the cladding and a short distance (up to 10 mm) into the base metal. The magnitude of the residual stress at the CBMI depends on the heat input during the cladding process, the subsequent stress relief and hydrostatic test conditions, and the operating temperature. The stress free temperature (SFT) is the temperature at which the residual stress at the CBMI is zero. As the operating temperature decreases below the SFT, the value of K_I for a small inner surface flaw increases, and at temperatures near room temperature, the applied K_I from the residual cladding stress can reach values from 15 to 20 ksi-√in (16.5 to 22 MPa-√m). Applied K_I values of this magnitude can produce a substantial increase in the potential for the extension of small inner surface flaws near the CBMI.

Several analyses have been performed in the U.S. to determine the SFT that is used to evaluate the effect of cladding in RPVs. In an early study [A-1], the SFT was determined to be approximately 400°F (204°C). This study considered the effect of the cladding process, and subsequent stress relief and hydrostatic test.

A second study [A-2] used a combination of finite element analyses and experimental data to determine the SFT; the results from this work determined that the SFT = 468°F (242°C). This analysis subsequently was updated to include temperature dependent material properties and determined that the SFT = 488°F (253°C), which was subsequently used [A-3] in the development of the Alternate PTS Rule. The SFTs determined from these two analyses were based on axial surface flaws. However, since the flaw distributions used with the FAVOR software contain only circumferential surface flaws, the SFT recently was recomputed for circumferential flaws using the same data and evaluation procedure described in [A-2], and it was determined that the SFT = 364°F (184°C) [A-4].

In other recent work [A-5], measured residual cladding stresses obtained from a study by the International Cooperative Program Network for Evaluation of Structural Components (NESC) were used to determine the cladding K_I, where the cladding residual stresses were measured at distances up to 0.55-inches (14-mm) (including cladding thickness = 0.25-inches) (6-mm) from the cladding surface into the base metal. The results from this work [A-5] indicate that the K_I obtained from the NESC measured residual stresses is about 10% lower than the K_I obtained using the SFT = 488°F (253°C).

The results reported in [A-5] were used to determine SFT that is equivalent to the cladding residual stress obtained from the NESC program. This evaluation was performed so a SFT consistent with the residual stresses obtained from the NESC program could be used in the FAVOR software to evaluate the integrity of forged components with postulated carbon macrosegregation.

Figure 6 in [A-5] presents a comparison of applied K_I time histories obtained from the NESC residual stresses with the applied K_I time histories obtained from a finite element analysis with SFT = 488°F (253°C) during a RPV cooldown from 532°F (278°C) to 70°F (21°C) at a rate of 50F/hr. (28°C/hr.). The applied K_I curves presented in Figure 6 of [A-5] include the thermal gradient stresses and cladding residual stresses for a circumferential, inner surface flaw with an infinite aspect ratio. Since the thermal gradient K_I is the same for both curves, then the difference between the two curves is the difference in the cladding K_I for SFT=488°F (253°C) and the NESC cladding residual stress distribution. This difference (measured manually from Figure 6 [A-5]) is approximately 1.8 ksi-√in (2 MPa-√m); consequently, the NESC cladding K_I is 1.8 ksi-√in (2 MPa-√m) less than the cladding K_I computed from FAVOR for SFT = 488°F (253°C).

Figure A-1 shows a comparison of the cladding K_I computed using FAVOR with SFT =488°F (black curve) and the NESC curve (dotted red curve), which is the FAVOR curve minus 1.8 ksi-√in (2 MPa-√m). The equivalent SFT for the NESC curve is defined by the SFT that provides the cladding K_I from FAVOR that will match the NESC curve. As shown in Figure A-1, the NESC curve is bounded above by the curve from FAVOR with SFT =450°F (232°C) and below by the curve from FAVOR with SFT = 440°F (227°C); this visual presentation shows the sensitivity of the cladding K_I to SFT and indicates that a SFT = 445°F (229°C) will provide a good match the NESC curve. Based on these results, a SFT = 445°F (229°C) was used in the PFM analyses to evaluate the integrity of forged components with postulated carbon macrosegregation.

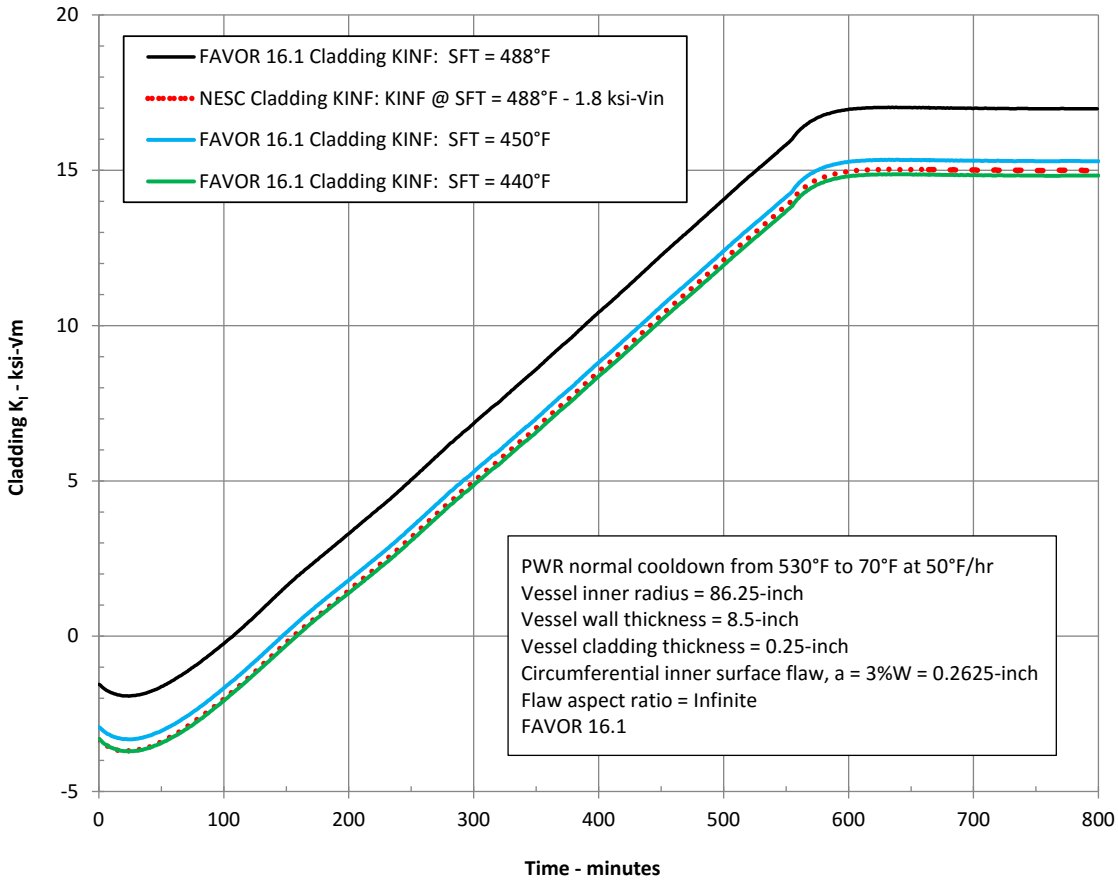

Figure A-1
Determination of FAVOR Equivalent SFT from Measured Residual Cladding Stresses for a Small Circumferential Inner Surface Flaw near the CBMI

References

A-1. Ganta, B.R., Ayres, D.J., and Hijeck, P. J., "Cladding Stresses in a Pressurized Water Reactor Vessel Following application of the Stainless Steel Cladding, Heat Treatment and Initial Service," ASME Pressure Vessel and Piping, Pressure Vessel Integrity, Vol. 213, pp. 245-252, 1991.

A-2. Dickson, T., et al., Evaluation of Margins in the ASME Rules for Defining the P-T Curve for a RPV, Proceedings of the Twenty-Sixth Water Reactor Safety Information Meeting NUREG/CP-0166, Vol. 1, October 26-28, 1998, (ADAMS Public Documents, Accession Number ML042230476).

A-3 P.T. Williams, T.L. Dickson, B.R. Bass, and H.B. Klasky, Fracture Analysis of Vessels – Oak Ridge FAVOR, v16.1, Computer Code: Theory and Implementation of Algorithms, Methods, and Correlations, ORNL/TM-2016/309, Oak Ridge National Laboratory, Oak Ridge, TN, September, 2016.

A-4. Dickson, T., and Bass, R., Impact of Using a Stress Free Temperature of 364°F on Shallow Flaw Issue, NRC Public Meeting on Reactor Pressure Vessel Issues, January 19, 2016, Rockville, Maryland, USA. (ADAMS Accession No. ML16021A008).

A-5. Kusnick, J., et al., Effect of Cladding Residual Stress Modeling Technique on Shallow Flaw Stress Intensity Factor in a Reactor Pressure Vessel, Proceedings of the ASME Pressure Vessels and Piping Conference, July 19-23, 2015, PVP2015-45086.

The Electric Power Research Institute, Inc. (EPRI, www.epri.com) conducts research and development relating to the generation, delivery and use of electricity for the benefit of the public. An independent, nonprofit organization, EPRI brings together its scientists and engineers as well as experts from academia and industry to help address challenges in electricity, including reliability, efficiency, affordability, health, safety and the environment. EPRI members represent 90% of the electric utility revenue in the United States with international participation in 35 countries. EPRI's principal offices and laboratories are located in Palo Alto, Calif.; Charlotte, N.C.; Knoxville, Tenn.; and Lenox, Mass.

Together...Shaping the Future of Electricity

Program:

Materials Reliability

3002010331

Electric Power Research Institute
3420 Hillview Avenue, Palo Alto, California 94304-1338 • PO Box 10412, Palo Alto, California 94303-0813 USA
800.313.3774 • 650.855.2121 • askepri@epri.com • www.epri.com